LBL-10652 c. 2
Preprint

Lawrence Berkeley Laboratory
UNIVERSITY OF CALIFORNIA

Physics, Computer Science & Mathematics Division

Submitted to Annual Reviews of Nuclear and Particle Science

CHARMED MESONS PRODUCED IN e^+e^- ANNIHILATION

Gerson Goldhaber and James E. Wiss

March 1980

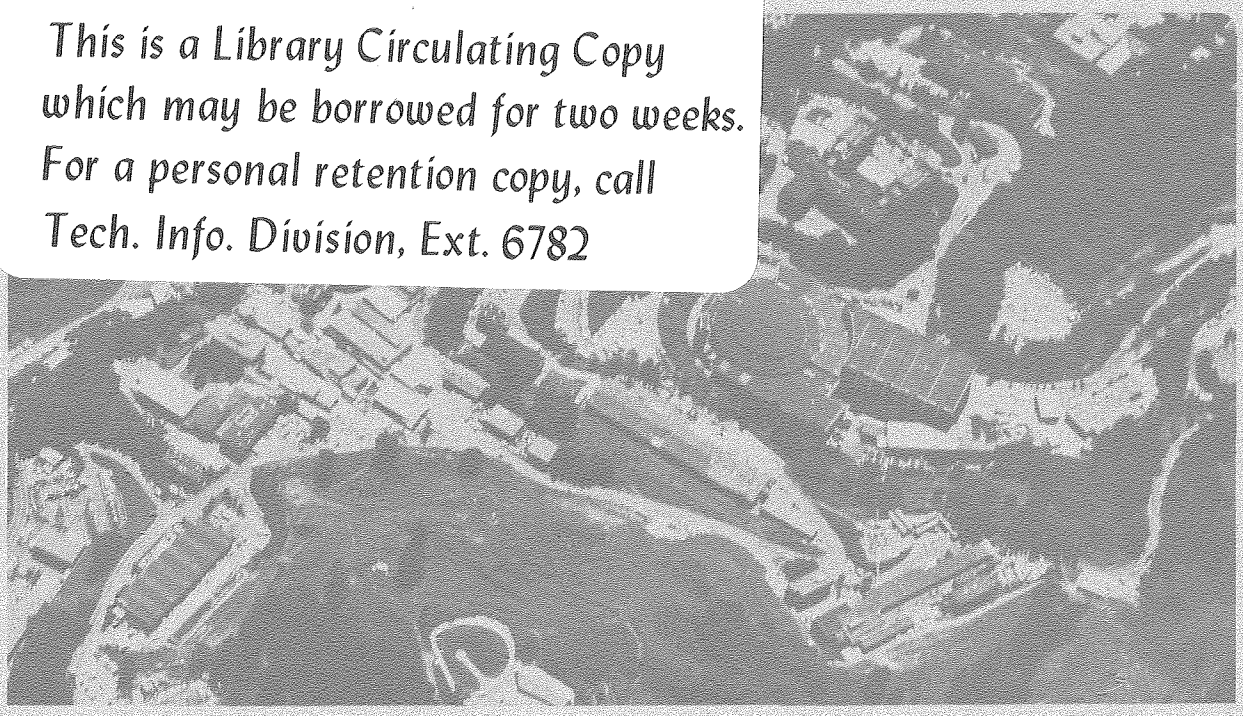

Prepared for the U.S. Department of Energy under Contract W-7405-ENG-48

DISCLAIMER

LBL-10652

CHARMED MESONS PRODUCED IN e^+e^- ANNIHILATION

Gerson Goldhaber
Department of Physics and Lawrence Berkeley Laboratory
University of California, Berkeley, California 94720

and

James E. Wiss
Department of Physics, University of Illinois, Urbana, Illinois 61801

CONTENTS

1. INTRODUCTION

The study of high-energy electron-positron annihilation has revealed a rich spectrum of new phenomena including the discovery of new, hadronically stable particles -- the charmed mesons. These particles are particularly interesting because they are the lightest particles containing the fourth quark and thus serve to test in a novel way many theoretical ideas about quarks and their interactions.

Prior to the general acceptance of the existence of charm, elementary particles were assumed to be constructed from three constituents or quarks. We shall employ the nomenclature up (u), down (d) and strange (s) for these three conventional quarks. Their quantum numbers are summarized in Table 1.1. This three-quark model for elementary particles, first proposed independently by Gell-Mann and Zweig in 1964, proved enormously successful in explaining the spectroscopy of the known hadrons, as well as many of the features of their interactions. Until the early 1970's there was little experimental need for a fourth quark. But then in 1970 Glashow, Illiopoulos & Maiani (GIM) demonstrated that the inclusion of a new quark, the charmed quark (c), would fix up a problem with the Weinberg-Salam model of the weak interaction -- the non-observation of the strangeness changing neutral current (Aronson 1970, Carithers 1973, Clark 1971, Klems, Hildebrand & Stiening 1970). The existence of a fourth quark, of course, implied the existence of numerous new particles. Using the quark model convention of constructing mesons from quark-antiquark pairs, one could anticipate the existence of $c\bar{u}$, $c\bar{d}$, $c\bar{s}$ and $c\bar{c}$ mesons. The lowest-lying states of these first three mesons have been dubbed the D^{o} $(c\bar{u})$, D^{+} $(c\bar{d})$, and the F^{+} $(c\bar{s})$, and are the subject of

this review. The family of mesons consisting of $c\bar{c}$, are known as the psions and their discovery in 1974 in conjunction with the discovery of charmed mesons in 1976 gave the first compelling evidence for the validity of the charm theory.

We shall begin our review by summarizing the first experimental indications for the existence of charm as obtained from experiments in e^+e^- annihilation. This will include a brief discussion of the role of charm in the understanding of the ψ mesons, as well as the unraveling of the intricate structure present in the e^+e^- total hadronic cross section. Next we shall discuss the discovery of the D^o, and D^+, and detail those properties crucial to their identification as charmed particles. Following will be a review of the properties of the D^o and D^+ learned through studies at the $\psi(3770)$ resonance. Compelling evidence will be summarized indicating that this state decays nearly exclusively into $D\bar{D}$, thus making it particularly useful in establishing inclusive and exclusive D branching fractions.

Our discussion of branching fractions will include two particularly important D decay modes, $D^o \to \pi^+\pi^-$ and $D^o \to K^+K^-$. These processes are suppressed relative to $D^o \to K^-\pi^+$ in the standard charm model, and thus serve as a critical test of that theory. This will be followed by a discussion of the D semileptonic decay modes which provide useful information on the D^o and D^+ lifetimes.

Turning our attention to the data collected beyond the $\psi(3770)$ we will discuss the properties and production mechanisms of the excited charm mesons, the D^{*o} and the D^{*+}. D production just above the $\psi(3770)$ appears to be dominated by the three quasi-two-body processes $e^+e^- \to D\bar{D}$,

$D^{*}\bar{D} + \bar{D}^{*}D$, and $D^{*}\bar{D}^{*}$, in accordance with early theoretical predictions. The relative amounts of each process, on the other hand, is somewhat surprising, and has lead to considerable theoretical speculation.

Finally, we will summarize evidence for the existence of the F meson which is as yet not on as solid a footing as the D^{o}, D^{+} isodoublet.

There has been a great deal of theoretical and experimental work on charmed particles within the last decade. Because of the limitations of space and time we will confine our review to the experimental aspects of charmed meson production through electron-positron annihilation. Hence we cannot review the many important results on production of charmed mesons by neutrino, photon, and hadron beams, or discuss the important results on charmed baryons. Our emphasis will be entirely on experimental matters. The theoretical aspects of charm have been recently reviewed in this series by Appelquist, Barnett & Lane (1978). When we have found it necessary to reference theoretical works, we have done so in the spirit of illustration and have made no attempt to be exhaustive or judgmental.

2. THE $e^{+}e^{-}$ ANNIHILATION PROCESS

2.1. QED and Nonresonant Annihilation

The electron-positron annihilation process has been studied using the colliding beam technique since the early 1960's (Schwitters & Strauch 1976). The early motivation for such experiments was first the study of QED process, such as $e^{+}e^{-} \rightarrow \mu^{+}\mu^{-}$, and $e^{+}e^{-} \rightarrow e^{+}e^{-}$, and later the study of $e^{+}e^{-} \rightarrow$ hadrons. Both processes are assumed to be dominated by the s-channel exchange of a virtual photon as illustrated in Fig. 2.1. The cross section for the process $e^{+}e^{-} \rightarrow \mu^{+}\mu^{-}$ (neglecting the mass of the muon and radiative corrections) is $\sigma(\mu\mu) = 4\pi\alpha^{2}/3s$ where $s = E^{2}_{c.m.}$. In analogy with Fig. 2.1(a) we expect

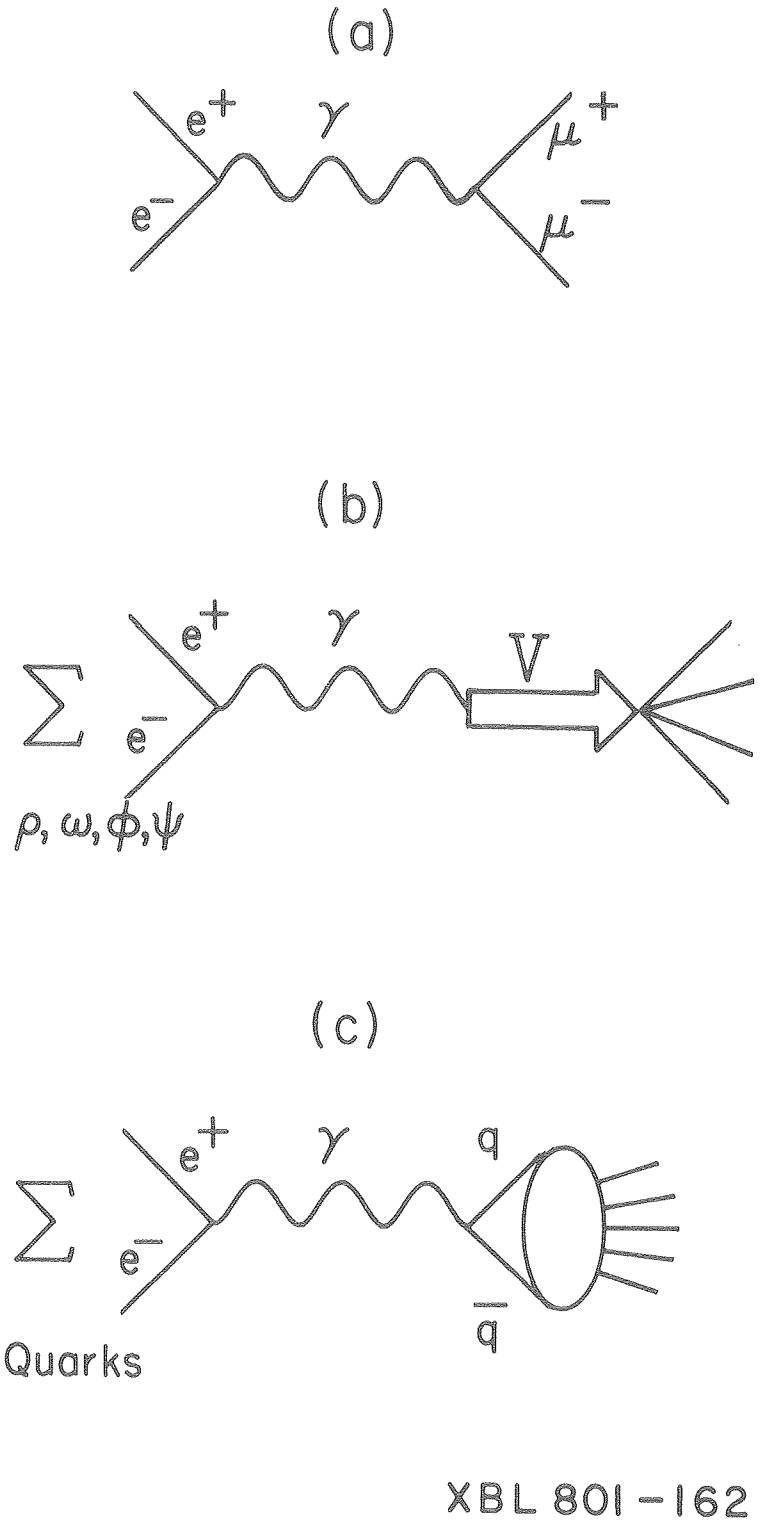

Figure 2.1. (a) The 1γ diagram for the QED process $e^+e^- \rightarrow \mu^+\mu^-$. Two types of 1γ contribution to $e^+e^- \rightarrow$ hadrons: (b) Hadronic decays of vector mesons. This should dominate when $\sqrt{s}$ is near the mass of the vector mesons. (c) Hadronic contribution from the point-like production of quarks.

$$\sigma_{had} = \frac{4\pi\alpha^2}{3s} \sum Q_i^2$$

where Q_i are the contributing quark charges, and i ranges over those flavors with quark masses $< \sqrt{s}/2$ and the three quark colors.

Below a center-of-mass energy of about 1.5 GeV, hadronic production by e^+e^- annihilation is dominated by the decays of vector mesons as shown in Fig. 2.1(b) with sizable contributions from the ρ, ω, and φ. Many of the beautiful results obtained in this region are summarized by Perez-y-Jorba (1969).

Early data collected beyond the ρ, ω and φ resonance region but below 3 GeV appeared to be consistent with the predictions of the naive pointlike parton model, as shown in Fig. 2.1(c). $\sigma_{hadronic}$ should scale in the limit of negligible quark masses (and small QCD corrections) as $1/s$. The traditional way of expressing this scaling behavior evokes the famous ratio,

$$R \equiv \sigma_{e^+e^- \to \text{hadrons}} / \sigma_{e^+e^- \to \mu^+\mu^-} \quad .$$

As illustrated in Figs. 2.1 the naive quark model prediction for this ratio is $R = \sum Q_i^2$.

Experimental measurements in the range $1.5 \lesssim E_{c.m.} \lesssim 3$ GeV taken prior to 1974 were consistent with values of R ranging from 2 to 3 (Richter 1974). Very recent data taken in this energy region by ADONE and DCI shows consistency with $R = 2$ with considerably smaller error bars (summarized by Feldman 1978).

The value of $R = 2$ is precisely what one would expect in the original three-quark model (quark charges of 2/3, -1/3, and -1/3) with the added color degree of freedom, whereby each quark is present in three colors.

As early as 1973, data accumulated at CEA indicated a rise in R to a value of 4.7 ± 1.1 nb at $\sqrt{s} = 4$ GeV (Litke 1973, Tarnopolsky 1974). This rise in R was later corroborated by the SLAC-LBL collaboration working at SPEAR (Richter 1974). Although initial theoretical response was varried (Ellis 1974), one hypothesis for the rise in R was the opening up of new degrees of freedom such as the threshold of a new quark, or the production of a new heavy lepton (Perl 1980). We now believe there were indeed contributions to R from both effects.

2.2. The Discovery of the J/ψ

The J/ψ was simultaneously observed in p Be collisions (Aubert 1974) and e^+e^- annihilations (Augustin 1974). In the hadronic production experiment the J appeared as a narrow enhancement in the electron pair invariant mass distribution in the reaction p Be $\rightarrow e^+e^-X$. This enhancement had a width of 20 MeV which was consistent with experimental resolution. The ψ was observed in e^+e^- annihilations as an enhancement in the total hadronic and lepton pair cross section for center-of-mass energies near the ψ mass of 3.095 ± 0.002 GeV, with a measured width compatible with their experimental resolution of 2 MeV.

Because the ψ appeared as an s-channel resonance in e^+e^- annihilation, one could make a precision width measurement using $\int \sigma(E)dE$ (where E is the center-of-mass energy and σ is the total resonant cross section) and the measured muon pair branching ratio of $\approx 7\%$, even though the total width was much smaller than the center-of-mass resolution of a storage ring. This analysis yielded the remarkable result $\Gamma_\psi = 69 \pm 15$ keV. The properties of known vector mesons are summarized in Table 2.1. Although the ψ is over three times as massive as the

conventional ρ, ω, and φ vector mesons, it is narrower by about two orders of magnitude.

Because of the anomalous ψ width, it was historically important to establish that the ψ was indeed a vector meson as implied by its s-channel production in e^+e^- annihilation. This prejudice was partially borne out through the observation of psi-photon interference in the process $e^+e^- \rightarrow \mu^+\mu^-$, which established the ψ quantum numbers as $J^{PC}(\psi) = 1^{--}$ (Boyarski 1975). In addition, data on the photoproduction of the ψ (Knapp 1975, Camerini 1975, Gittleman 1975) demonstrated that the ψ-nucleon total cross section was $\simeq$ 1 mb -- the same order of magnitude as the conventional vector mesons.

A search for additional narrow vector mesons formed in e^+e^- annihilation found the $\psi(3684)$ or ψ' with a width of 238 keV, the $\psi(4400)$ with a width of 33 ± 10 MeV, and considerably later, the $\psi(3770)$ with a width of 25 MeV.

As seen in Fig. 2.2 these resonances occur in the region where R makes a transition from a value of $\simeq 2.5$ to a plateau around 5.

THE OZI RULE AND THE ψ. The discovery of the new narrow vector meson states gave considerable encouragement to the proponents of a new quark. In fact such states were being predicted by charm enthusiasts concurrently with the experimental observation of the ψ (Appelquist, Barnett & Lane 1978). Within the charm picture the new vector mesons were assumed to be constructed from ^3S or ^3D states of $c\bar{c}$. Many such vector mesons can be constructed in the theory by placing the new quarks in various levels of radial excitation. The narrow width of the ψ could be explained as a manifestation of the phenomenological OZI rule (Okubo

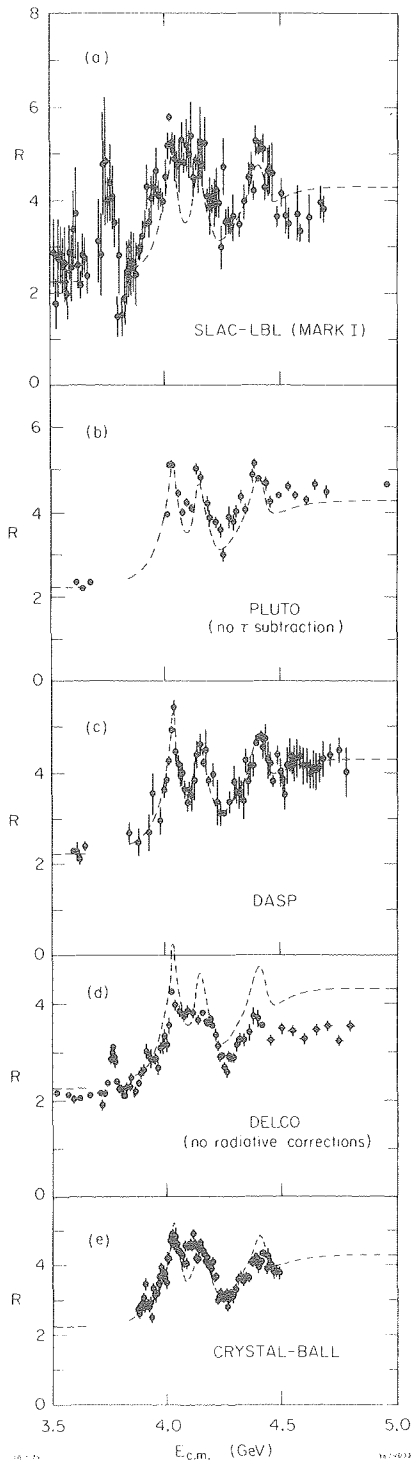

Figure 2.2. The observed values of R near charm threshold. All data are corrected for radiative effects and contamination from the τ, unless otherwise indicated. The hand-drawn curve, which follows the DASP points, has been applied to the other measurements in order to facilitate a comparison. Systematic errors, which range from 10 - 15%, are not included in the error-bars. (Summary by Kirkby 1979)

1963, Zweig 1964, Iizuka 1966) which was previously proposed to explain the suppression of certain strong interaction processes which can only occur via "disconnected" quark diagrams.

A disconnected diagram allows at least one external particle to be isolated by making a cut which does not intersect any quark line. For example, Fig. 2.3 demonstrates that $\varphi \to \pi^+\pi^-\pi^o$ proceeds via a disconnected or OZI-suppressed diagram, whereas $\varphi \to K^+K^-$ does not. Experimentally one does find that the decay $\varphi \to K\bar{K}$ is preferred over $\varphi \to \pi^+\pi^-\pi^o$, even though the former process has a much smaller phase space than the latter.

Using this rule one could explain the narrow widths of the ψ and ψ' by asserting that they had masses <u>below</u> the threshold for the pair production of the lowest-lying states (presumably D's) containing the new quark. If this were true, <u>all</u> decay diagrams for the ψ and ψ' would be disconnected and hence suppressed.

The dramatic increase in the width of the $\psi(4400)$, and as determined much later the $\psi(3770)$, would then represent the opening up of the $D\bar{D}$ decay channel. Hence one would expect the relation:

$$\frac{M\psi'}{2} < M_D < \frac{M\psi(3770)}{2}$$

or $1.842 < M_D < 1.885$ GeV, with the upper bound coming through considerable hindsight.

PROPERTIES OF THE ψ. If the psion family were comprised of $q\bar{q}$ states of a new quark, one would expect the presence of strongly decaying states of $J^{PC} \neq 1^{--}$ as well. These states would be constructed from P-wave or ^3S radial excitations of the new quark. Several such additional states have been observed via radiative decays from the ψ'. The beautiful

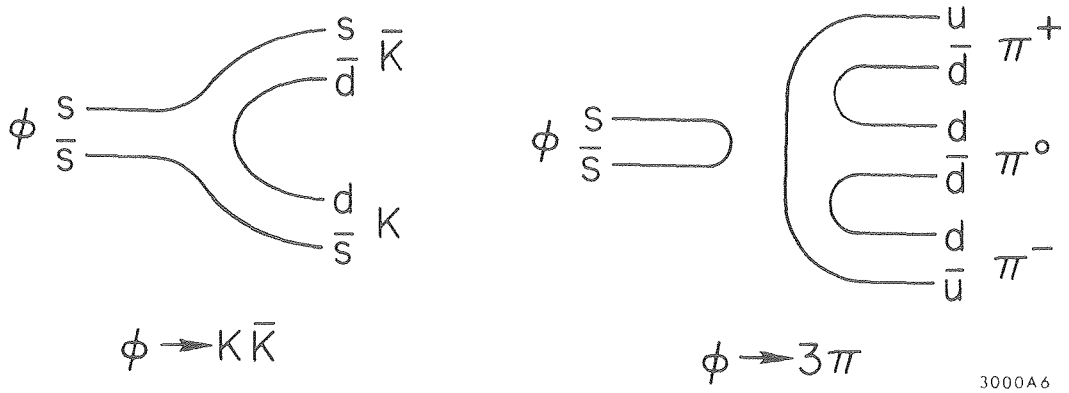

Figure 2.3. Illustration of OZI-allowed ($\varphi \rightarrow K\bar{K}$) and -forbidden ($\varphi \rightarrow \pi\pi\pi$) decays of the φ meson.

phenomenology associated with the many $c\bar{c}$ states below the charm threshold has been previously reviewed (Chinowsky 1977) and hence we will not discuss it here. Suffice it to say, however, that it is indeed difficult to account for the multitude of new narrow states produced in e^+e^- without accepting the presence of a new quark.

Additional evidence for this interpretation of the new mesons comes from a study of the ψ decay modes. We have previously noted that the OZI explanation for the narrow width of the ψ and ψ' implies the existence of a fourth quark. The large mass of the ψ suggests that this fourth quark is much heavier than the conventional three quarks, and hence if the new states consisted of quark-antiquark combinations of the new quark they must be isosinglet states.

A study of pion multiplicities in the decays of the ψ demonstrated that it has odd G-parity and thus (in light of its odd C-parity) the ψ has even isospin (Jean-Marie 1976).

Even isospin, coupled with the observation of a substantial $\psi \rightarrow p\bar{p}$ decay mode, proves that the ψ is an isosinglet as expected. Corroborating evidence comes from the observation of a $\Lambda\bar{\Lambda}$ decay mode (Peruzzi 1978).

To summarize, the observation and properties of the new mesons discovered in e^+e^- annihilation provides a vast body of data which is easily accommodated into the framework of a new, heavy quark. However there is little to link this quark to the charm quark of the GIM model from a study of the ψ family alone. The definitive proof of the charm hypothesis comes from the observation of states of nonzero charm -- the D^o and D^+. We turn now to a brief discussion of the properties one would expect in the GIM model for these mesons.

3. CHARM

3.1. The GIM Model

Several excellent and comprehensive reviews have been written concerning the theoretical aspects of charm since the seminal review of Gaillard, Lee & Rosner (1975). In this section we wish to outline those aspects of the theory necessary for the understanding of the experimental material to follow.

As we have previously stated, the charmed quark was partly motivated to provide a means of cancelling first-order strangeness changing neutral current effects such as $K_\ell \rightarrow \mu^+\mu^-$ and a first-order weak $K_s - K_\ell$ mass difference. In Fig. 3.1 we show a diagram for these processes within the three-quark theory. Although these diagrams appear to contribute to the second-order weak interaction, the loop integral enhances their strength making them comparable to a first-order diagram. The factors appearing at the diagram vertices follow from the form of the precharm weak hadronic current or:

$$J_h^\mu = \bar{u}\gamma^\mu(1 + \gamma^5)(d \cos\theta_c + s \sin\theta_c) \qquad (3.1)$$

where θ_c is the Cabibbo angle, introduced in 1963 to relate the strength of strangeness-conserving weak current to the strangeness-changing weak current. Present measurements indicate that the Cabibbo angle is small ($\theta_c = 13.2 \pm 0.5^\circ$).

Figure 3.2 shows alternative diagrams for the processes employing the charmed quark in place of the up quark. These diagrams will tend to cancel the diagrams of Fig. 3.1 provided the new vertex factors are as shown -- that is if Eq. 3.1 is modified to:

$$J_h^\mu = (\bar{u}\ \bar{c})\gamma^\mu(1 + \gamma^5) \begin{pmatrix} \cos\theta_c & -\sin\theta_c \\ \sin\theta_c & \cos\theta_c \end{pmatrix} \begin{pmatrix} d \\ s \end{pmatrix} \qquad (3.2)$$

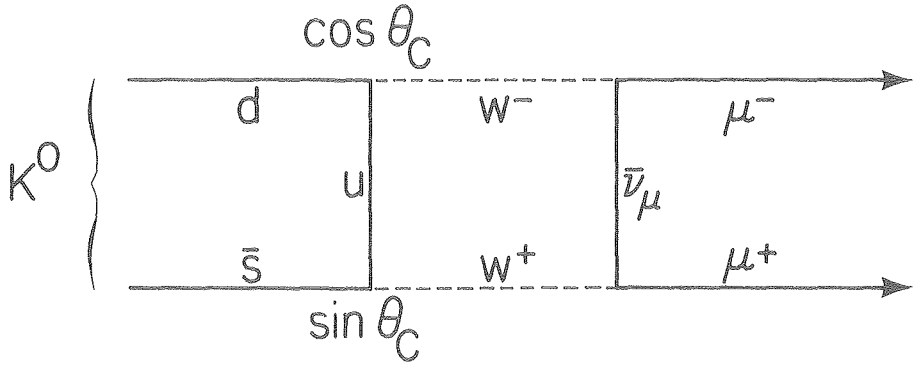

(a) $K_L^0 \rightarrow \mu^+\mu^-$ Decay

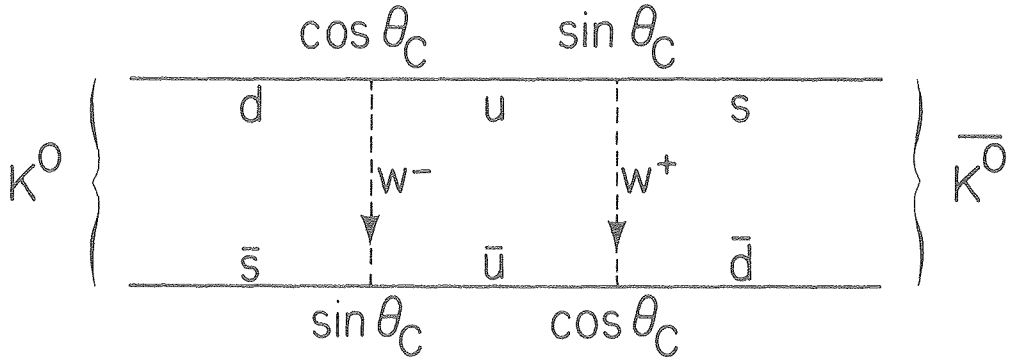

(b) K_L^0-K_S^0 Mass Splitting

XBL 791-288

Figure 3.1. Quark diagrams for the decay $K_L^0 \rightarrow \mu^+\mu^-$ and the K_L^0/K_S^0 mass splitting.

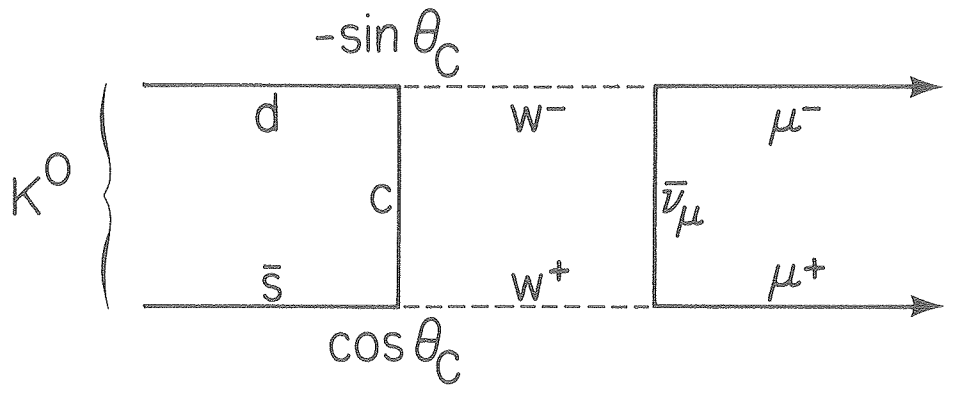

(a) $K_L^0 \rightarrow \mu^+\mu^-$ Decay

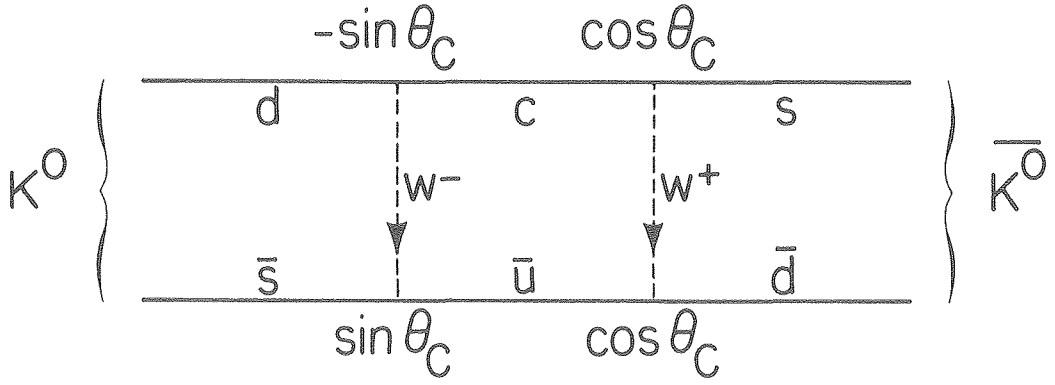

(b) K_L^0-K_S^0 Mass Splitting

XBL 791-290

Figure 3.2. Cancelling quark diagrams for the decay $K_L^0 \rightarrow \mu^+\mu^-$ and the K_L^0/K_S^0 mass splitting in the GIM model.

Equation 3.2, employing two quark doublets and a unitary mixing matrix is the hadronic current of the 1970 Gim model (Glashow 1970).

3.2. Predicted Decays of Charmed Mesons

Using Eq. 3.2 and the bilinear weak Lagrangian $L = J^{\dagger\mu} J_\mu + J^\mu J^\dagger_\mu$, one obtains the results of Tables 3.1 and 3.2 which list the flavor structure and Cabibbo-angle factors for the decays of charmed mesons expected in the GIM model.

As illustrated in the tables, one expects a wide disparity in rates between Cabibbo-favored decays such as $D^o \to K^- \pi^+$ or $D^o \to K^- e\nu$, singly-suppressed decays such as $D^o \to \pi^+\pi^-$ or $D^o \to \pi e\nu$, and doubly-suppressed decays such as $D^o \to K^+\pi^-$, owing to the smallness of the Cabibbo angle. We will compare the predictions of Table 3.1 and 3.2 to the data in Section 4.

3.3. Beyond Charm

Since the 1977 discovery of the Υ by Lederman and collaborators (Herb 1977), considerable indirect evidence has accumulated for the existence of another quark, the b quark, which is considerably more massive (~ 5 GeV) than the c quark. The simplest extension of the Weinberg-Salam, GIM model involves the introduction of a new quark doublet (t, b) where the b quark is the charge -1/3 lighter quark responsible for the Υ and the t quark is the heavier quark of charge 2/3 whose presence is still speculation.

The model of Kobayashi & Maskawa (1973) incorporates this new doublet into the weak current by proposing that the u, c, t quarks mix with the d, s, b quarks via a general unitary 3×3 mixing matrix. Hence:

$$J_h^\mu = (\bar{u}\,\bar{c}\,\bar{t})\,\gamma^\mu(1+\gamma^5)M\begin{pmatrix} d \\ s \\ b \end{pmatrix}$$

where

$$M = \begin{pmatrix} C_1 & -S_1C_3 & -S_1S_3 \\ S_1C_1 & C_1C_2C_3 - S_2S_3e^{i\delta} & C_1C_2S_3 + S_2C_3e^{i\delta} \\ S_1S_2 & C_1S_2C_3 + C_2S_3e^{i\delta} & C_1S_2S_3 - C_2C_3e^{i\delta} \end{pmatrix}$$

and $C_i = \cos\theta_i$, $S_i = \sin\theta_i$, $i = 1,2,3$.

Within this picture the single Cabibbo angle present in the Eq. 3.2 (now called θ_i) is augmented by two new angles θ_2 and θ_3 and a phase factor ($e^{i\delta}$). We note that the original GIM predictions for the weak transitions between the u, d, s and c quarks are recovered in the limit $\theta_2, \theta_3 \to 0$.

Nonzero values for the new mixing angles will affect both the weak decays of conventional particles as well as the decays of charmed particles. In particular, we see that the Cabibbo-suppressed processes $D^o \to \pi^+\pi^-$ and $D^o \to K^+K^-$ will no longer have identical mixing angle factors as was the case in the GIM model. Within the sector of older phenomena, we see that the predictions for processes involving $u \rightleftarrows d$ transitions such as neutron beta decay still involve only the original Cabibbo angle θ_1. We can thus retain the value $\theta_1 = 13.2 \pm 5^o$ as measured by the reaction $n \to pe\bar{\nu}$.

The amplitude for $u \rightleftarrows s$ transitions, however, acquires a new mixing factor becoming $\sin\theta_1 \cos\theta_3$. The success of the original Cabibbo model applied to processes such as $\Lambda \to pe\bar{\nu}$ and $K \to \pi e\nu$ thus limits the Kobayashi-Maskawa correction to $|\cos\theta_3| > 0.87$ (Schrock & Wang 1978). Less direct theoretical arguments based on the

possible contributions of the t quark to the $K_\ell - K_s$ mass difference set a limit of $\theta_2 < 30^\circ$ (Harari 1977). These limits, when applied to the D decays can cause deviations from the GIM predictions by factors of two although the basic pattern of enhanced vs suppressed decays would be expected to hold.

4. D MESONS

4.1. Discovery of D Mesons

D mesons were first observed by the SLAC-LBL Mark I collaboration at SPEAR in 1976 using data collected at center-of-mass energies ranging from 3.9 to 4.6 GeV (Goldhaber 1976 and Peruzzi 1976). The first D decay modes observed included $D^0(1863) \rightarrow K^-\pi^+$, $K^-\pi^+\pi^+\pi^-$ and $D^+(1868) \rightarrow K^-\pi^+\pi^+$. A substantial body of evidence soon accumulated linking the narrow enhancements in the $K^-\pi^+$, $K^-\pi^+\pi^+\pi^-$, and $K^-\pi^+\pi^+$ invariant mass distributions to the D^0, D^+ charmed isodoublet. We outline the evidence below:

EVIDENCE FOR ASSOCIATED PRODUCTION. Both the $D^0(1863)$ and $D^+(1868)$ are produced in final states containing a $D\bar{D}$ pair as one would expect for particles containing a quantum number conserved by the electromagnetic interaction. This is evidenced by two observations:

(a) No D's are observed in e^+e^- annihilation at either the ψ or ψ', although a substantial amount of Mark I data was collected at these resonances. The ψ' in particular is located just below $D\bar{D}$ threshold.

(b) No evidence is seen in recoil mass spectra against the D^0 or D^+ system for events with recoil masses smaller than the D candidate mass of 1863 MeV.

EVIDENCE FOR WEAK HADRONIC DECAYS. Particles carrying a quantum number conserved in the strong or electromagnetic interaction must decay

weakly. This is evidenced by five observations:

Narrow width. All reported sightings of the D^0 and D^+ into inclusive decay modes report an observed width which is consistent with experimental mass resolutions. The data with the best mass resolution sets a limit $\Gamma_{D^0,D^+} < 2$ MeV.

Parity violation. The observation of parity violation in the decays $D^0 \to K^-\pi^+$ and $D^+ \to K^-\pi^+\pi^+$ is reminiscent of the θ-τ problem for K decays of the 1950's, which led to the hypothesis of a parity violating weak interaction. Because of the small mass difference between the $D^0(1863)$ and $D^+(1868)$ it is natural to assume that they are members of the same isodoublet and hence have the same spin and parity. The $D^0 \to K\pi$ decay final state must have a natural spin parity of 0^+, 1^-, 2^+, ... A study of the $D^+ \to K^-\pi^+\pi^+$ Dalitz plot (Wiss 1976) rules out D^+ final-state spin-parity assignments of $J^P = 1^-$ and 2^+, while 0^+ is forbidden by angular momenta considerations for three pseudoscalars. Hence neglecting possible higher spin assignments for the D system one is left with a contradiction which can most naturally be resolved by assuming that the D^0 and D^+ decay through the parity-violating weak decay.

An exotic final state. Because of the $\Delta S = \Delta Q$ selection rule for the Cabibbo-favored hadronic decays of charmed particles, the D^+ must always decay hadronically into final states of positive charge and negative strangeness. Within the context of the conventional three-quark model such final states are labeled as "exotic" because they cannot be constructed from quark-antiquark pairs using the u, d, or s quarks. Hence if the $K^-\pi^+\pi^+$ enhancement at 1863 MeV which we implicitly associate with

the weak decay $D^+ \to K^-\pi^+\pi^+$ actually represented the strong decay of a noncharmed meson, that meson would be exotic, and would be the first compelling observation of such a state. The observation of the $I_z = 3/2$ $K^-\pi^+\pi^+$ enhancement when combined with the non-observation of an enhancement in $K^-\pi^+\pi^-$, the $I_z = -1/2$ brother, rules out such an interpretation, however.

Semileptonic decay. The observation of an appreciable semileptonic branching ratio, as discussed below, again suggests that D's do not decay strongly.

Evidence for a GIM pattern of decays. The Cabibbo-suppressed decay modes $D^0 \to K^-K^+$ and $\pi^+\pi^-$ have recently been observed in the SLAC-LBL Mark II detector at SPEAR. The dominant two-body decay mode, however, is $D^0 \to K^-\pi^+$. Hence the D^0 is observed to decay into both strange and nonstrange final states which implies that the decay mechanisms do not conserve strangeness and are thus weak. As we have previously discussed this pattern of decay modes is characteristic of charm in the GIM model.

Much of the information presented above linking the early $(K\pi)^0$, $(K3\pi)^0$, and $(K2\pi)^+$ signals to the D^0D^+ charmed doublet was performed at the Mark I detector using data collected from 3.9 - 4.6 GeV with an emphasis on the 4.028-GeV resonance region. Although charmed mesons are copiously produced near 4.028 GeV, the considerable structure in the total cross section near this enhancement precludes a clean Breit-Wigner fit to determine the cross section beneath the peak. Such information would have been useful, for, as we shall discuss shortly, it provides a means of measuring the absolute branching fractions for the D decay modes.

4.2. Hadronic Decays of D Mesons

THE $\psi(3770)$ RESONANCE. Following the end of data taking by the Mark I at SPEAR, the $\psi(3770)$ or ψ'' resonance was discovered in the LGW and DELCO experiments (Rapidis 1977 and Bacino 1978). Comparing the width of the ψ', Γ = 228 keV, with that of the ψ'', Γ = 25 MeV, we note that the effect of the OZI suppression at the ψ' is no longer present at the ψ'', since it lies above $D\bar{D}$ threshold. Furthermore the ψ'' lies below DD^* threshold and hence it can only decay into D's via the process $D^0\bar{D}^0$ or D^+D^-.

The ψ'' has been studied extensively in the LGW and DELCO experiments and recently again in the SLAC-LBL Mark II experiments (Lüth 1979, Schindler 1980). Figure 4.1 shows the R distribution observed in the Mark II experiment, where R is the ratio of the observed hadronic cross section to the theoretical QED μ-pair cross section $\sigma_{\mu\mu}$. The latter is obtained from calibration against observed Bhabha pairs. Figure 4.1(a) gives the R distribution where the $\tau^+\tau^-$ cross section has been subtracted. Figure 4.1(b) gives the R distribution after the radiative tails from the J/ψ and ψ' have been subtracted as well. The errors shown are statistical. The resonance is fitted to a p-wave Breit-Wigner expression (Barbaro-Galtieri 1968) with an energy-dependent total width $\Gamma_{tot}(E_{c.m.})$ which takes account of closeness to the different $D^0\bar{D}^0$ and D^+D^- thresholds. The explicit fitting function employed is:

$$R(E_{c.m.}) = \frac{1}{\sigma_{\mu\mu}} \frac{3\pi}{M^2} \frac{\Gamma_{ee}\Gamma_{tot}(E_{c.m.})}{(E_{c.m.} - M)^2 + \Gamma^2_{tot}(E_{c.m.})/4} \qquad (4.1)$$

and

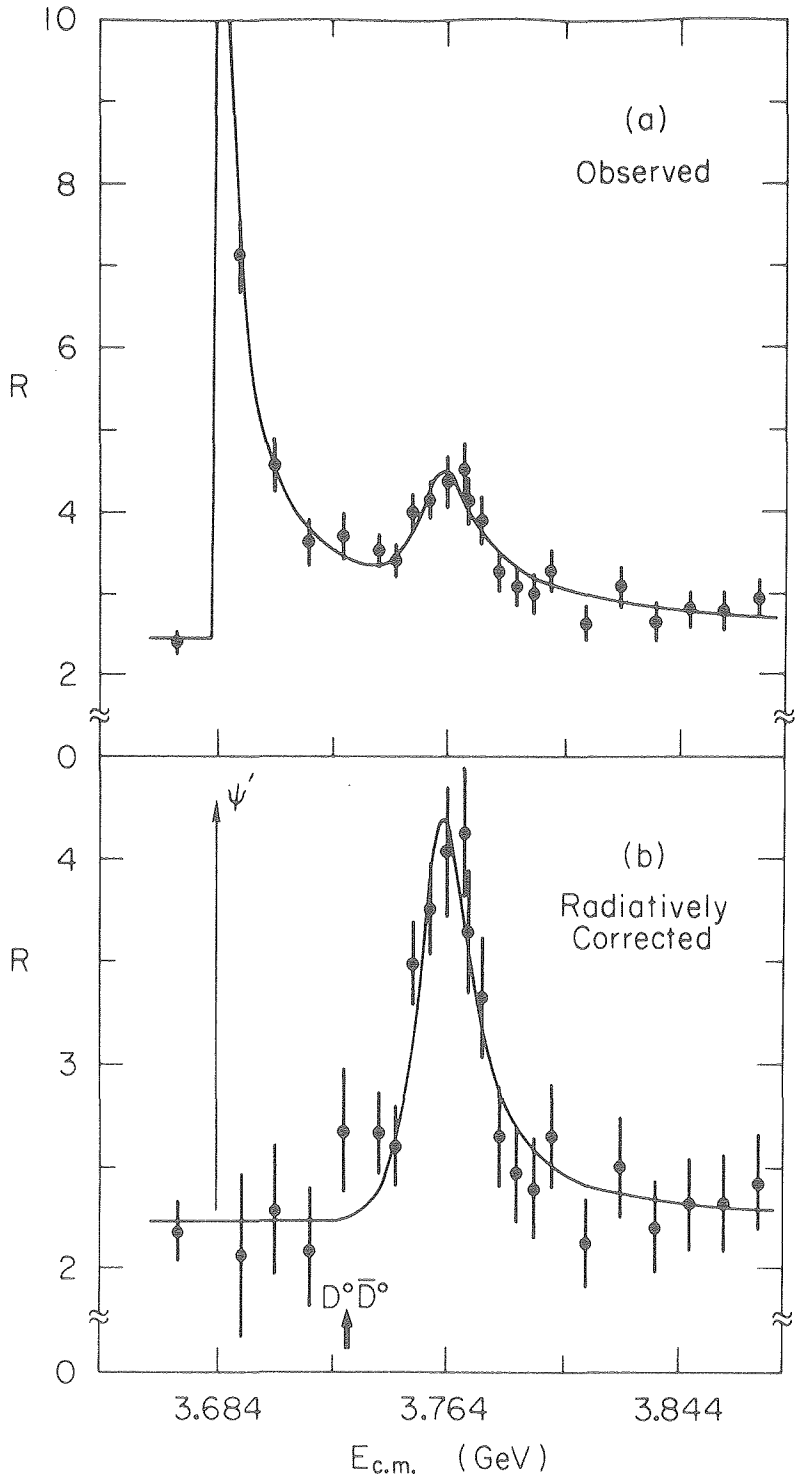

XBL 801-7877

Figure 4.1. The value of $R \equiv \sigma_{had}/\sigma_{\mu^+\mu^-}$ in the vicinity of the ψ'' obtained by the Mark II Collaboration (Schindler 1980), (a) before and (b) after radiative correction using the technique of Jackson & Scharre (1975). The curve is a fit of the data to Eq. (4.1).

$$\Gamma_{tot}(E_{c.m.}) \propto \frac{p_+^3}{1 + (rp_+)^2} + \frac{p_o^3}{1 + (rp_o)^2}$$

where p_+ (p_o) is the momentum of the pair produced D^+ (D^o) and r the interaction radius. The quantities M (the resonance mass) and Γ_{ee} (the partial width to electrons) were additional free parameters. The fit is not sensitive to r which was fixed at 2.5 Fermi. Table 4.1 summarizes the results of this fit for the various experiments. We note that the Mark II results are consistent with those of DELCO and the LGW except for a shift in the central mass that is 6 - 8 MeV lower than previous values. In addition the Mark II value for the width of the decay into e^+e^- of 276 ± 50 eV lies in between the earlier reported values.

From theoretical arguments (Eichten 1976, Lane 1976, Gottfried 1978) the ψ'' is believed to be a $^3D_1$ state of charmonium which is however mixed with the ψ', the 2^3S_1 state. The relatively large Γ_{ee} value gives an estimate for this mixing angle of $20.3^o \pm 2.8^o$.

CHARMED MESON BRANCHING RATIOS. Without knowledge of the total D production cross section it is difficult to measure the branching ratio for a given exclusive final state. One can, however, readily measure the product σBr by counting the number of events observed in a given channel and dividing by the acceptance and luminosity. Charm production at the ψ'' offers the considerable advantage that $\sigma(D\bar{D})$ can be determined if one is willing to assume that:

(1) The ψ'' is a state of definite isospin (0 or 1); this allows a prediction of the D^o/D^+ production ratio, namely $\sigma(D^o)/\sigma(D^+) \simeq p_o^3/p_+^3$

as expected for p-wave production. This reflects the D^o and D^+ mass difference (1863.3 MeV and 1868.3 MeV respectively).

(2) The ψ'' decays nearly entirely into $D\bar{D}$ ($\sim$ 99%). This is based on the $\Gamma_{tot}(\psi')$ to $\Gamma_{tot}(\psi'')$ ratio ($\sim$ 1/100); i.e., that the OZI-suppressed portion of the ψ'' decay width is of the same magnitude as the $\Gamma_{tot}(\psi')$.

Assumption (2) has been tested with limited statistical accuracy using events where both members of a $D\bar{D}$ pair are observed decaying into exclusive final states. The D branching ratio obtained by this technique can be used to compute the absolute D production cross section at the ψ'' (Schindler 1979).

Using these assumptions and their fit to the radiatively corrected ψ'' resonance shape, the LGW collaboration determined that the $D^o\bar{D}^o$, and D^+D^- cross section averaged over their particular set of ψ'' running energies was 11.5 ± 2.5 nb and 9.1 ± 2.0 nb, respectively (Peruzzi 1977). Most of this running was done within 2 MeV of their nominal ψ'' mass. The Mark II, on the other hand, collected 49,000 hadronic events at an energy 7 MeV above their nominal ψ'' mass. They find that the total $D^o\bar{D}^o$, D^+D^- cross sections for their running conditions are 7.8 ± 1.2 nb and 5.9 ± 1.0 nb respectively (Schindler 1979).

The beam-constrained mass distribution obtained for several D^o and D^+ final states are shown in Fig. 4.2 for the LGW data and Figs. 4.3-4.5 for the Mark II data. The beam-constrained mass M_b is calculated using the relationship:

$$M_b = \sqrt{E_b^2 - p^2}$$

where E_b is the storage-ring single-beam energy and p is the momentum of the D^o, D^+ candidate as determined by the magnetic detector. Such

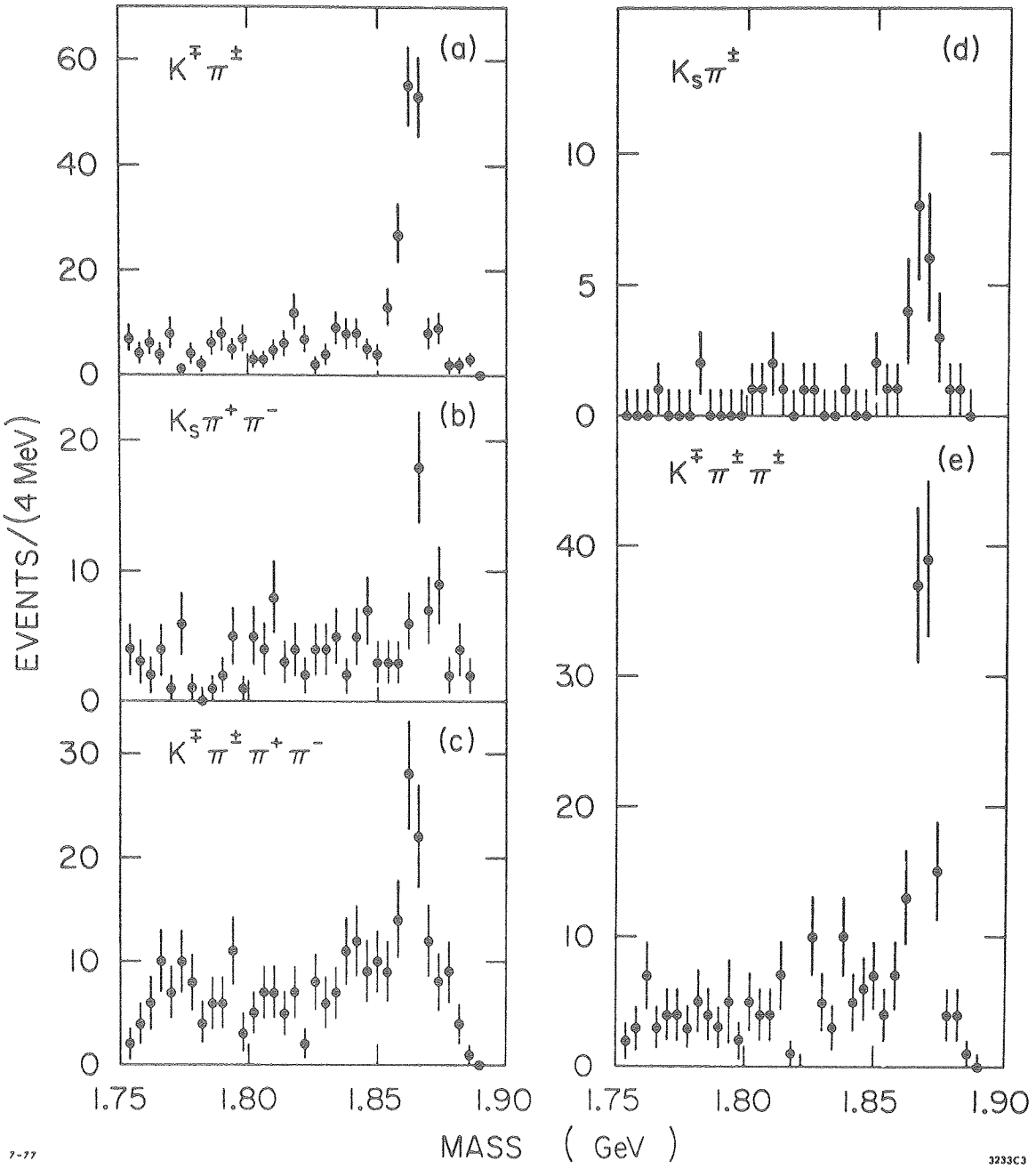

XBL 7711-10397

Figure 4.2. The beam-energy-constrained mass distributions for the indicated D^0, D^+ decay modes obtained by the LGW Collaboration at the ψ''.

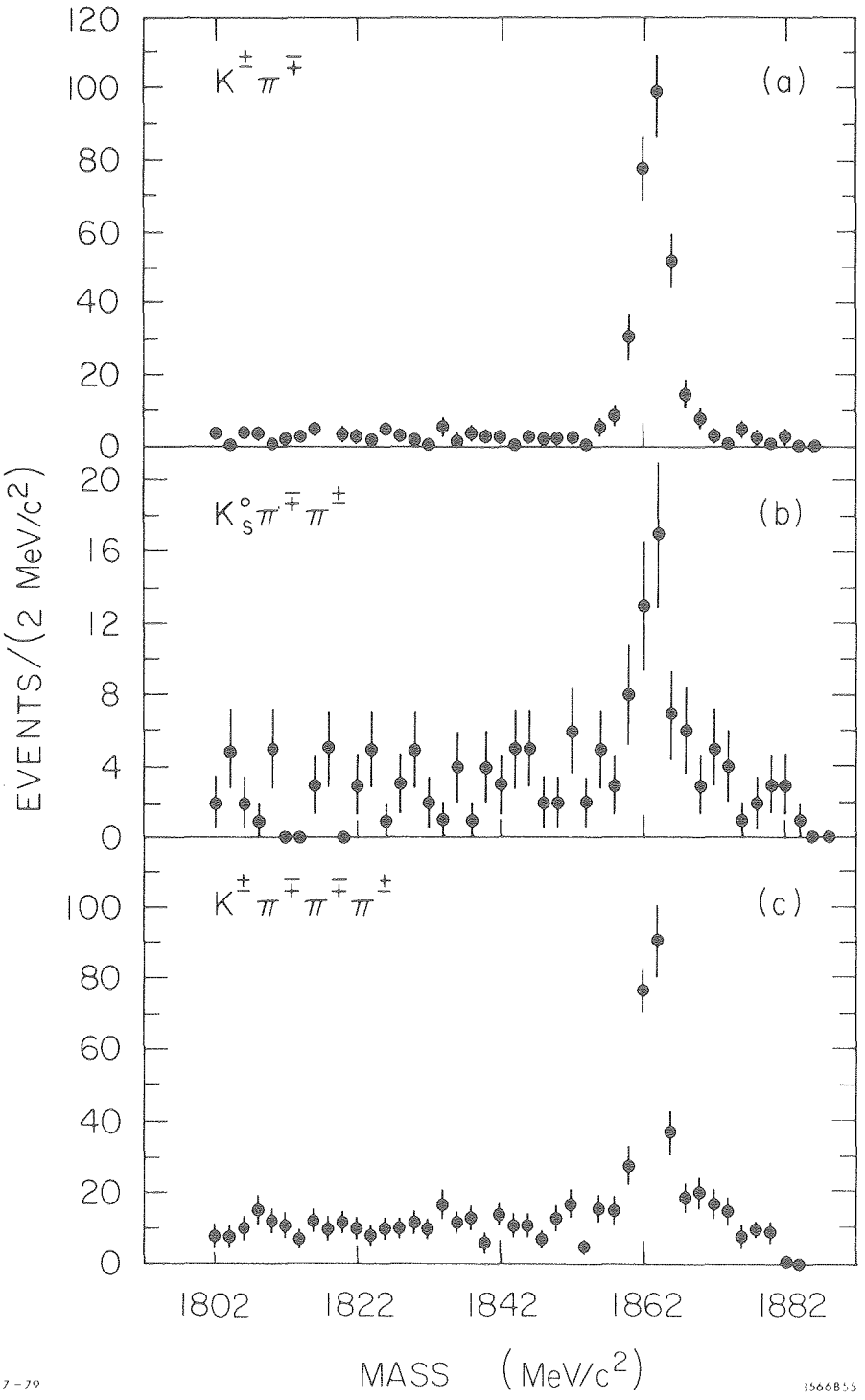

XBL 801-7867

Figure 4.3. Several D° beam-energy-constrained mass distributions obtained by the Mark II Collaboration at the ψ''.

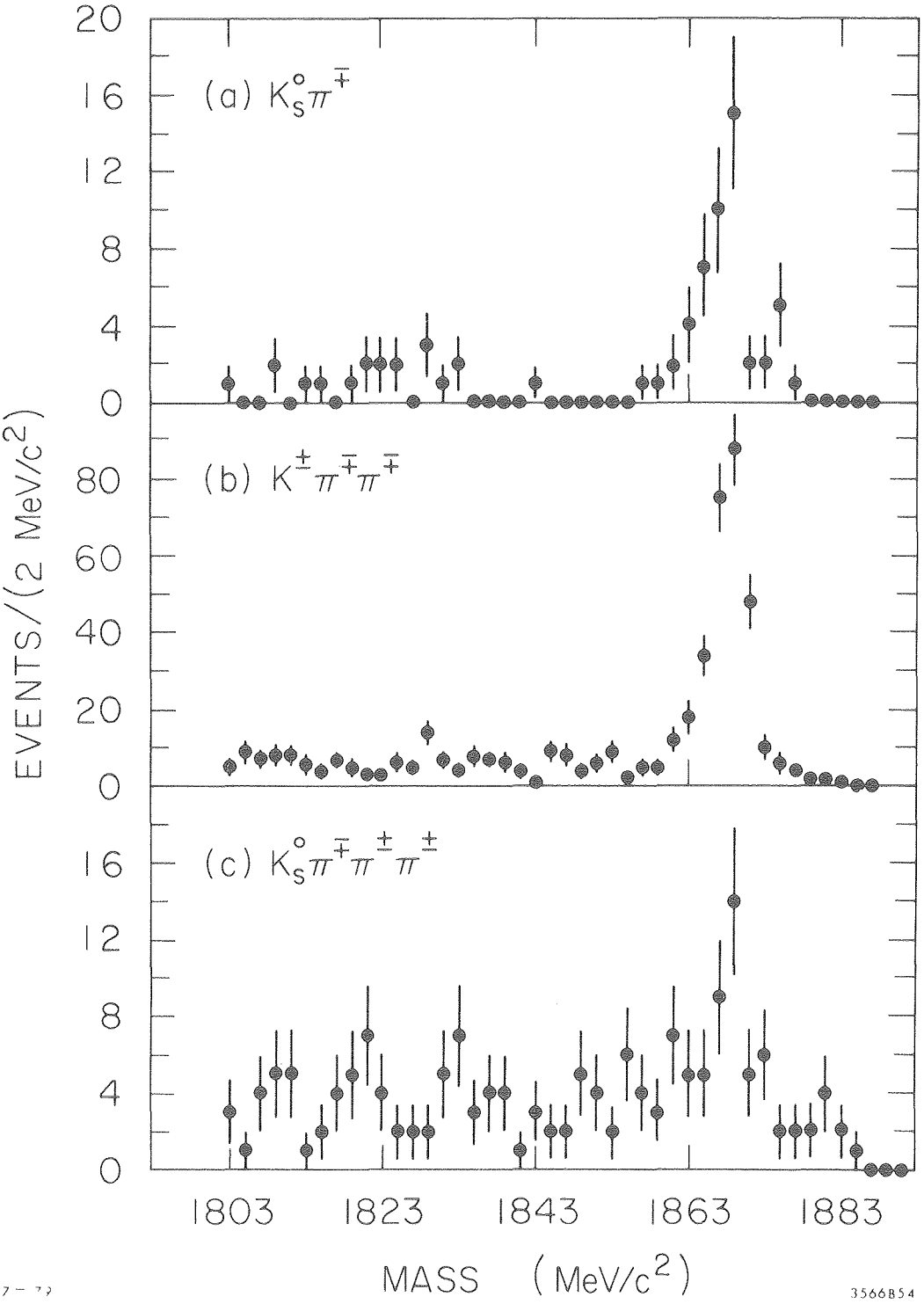

XBL 801-7866

Figure 4.4. Several D^+ beam-energy-constrained mass distributions obtained by the Mark II Collaboration at the ψ''.

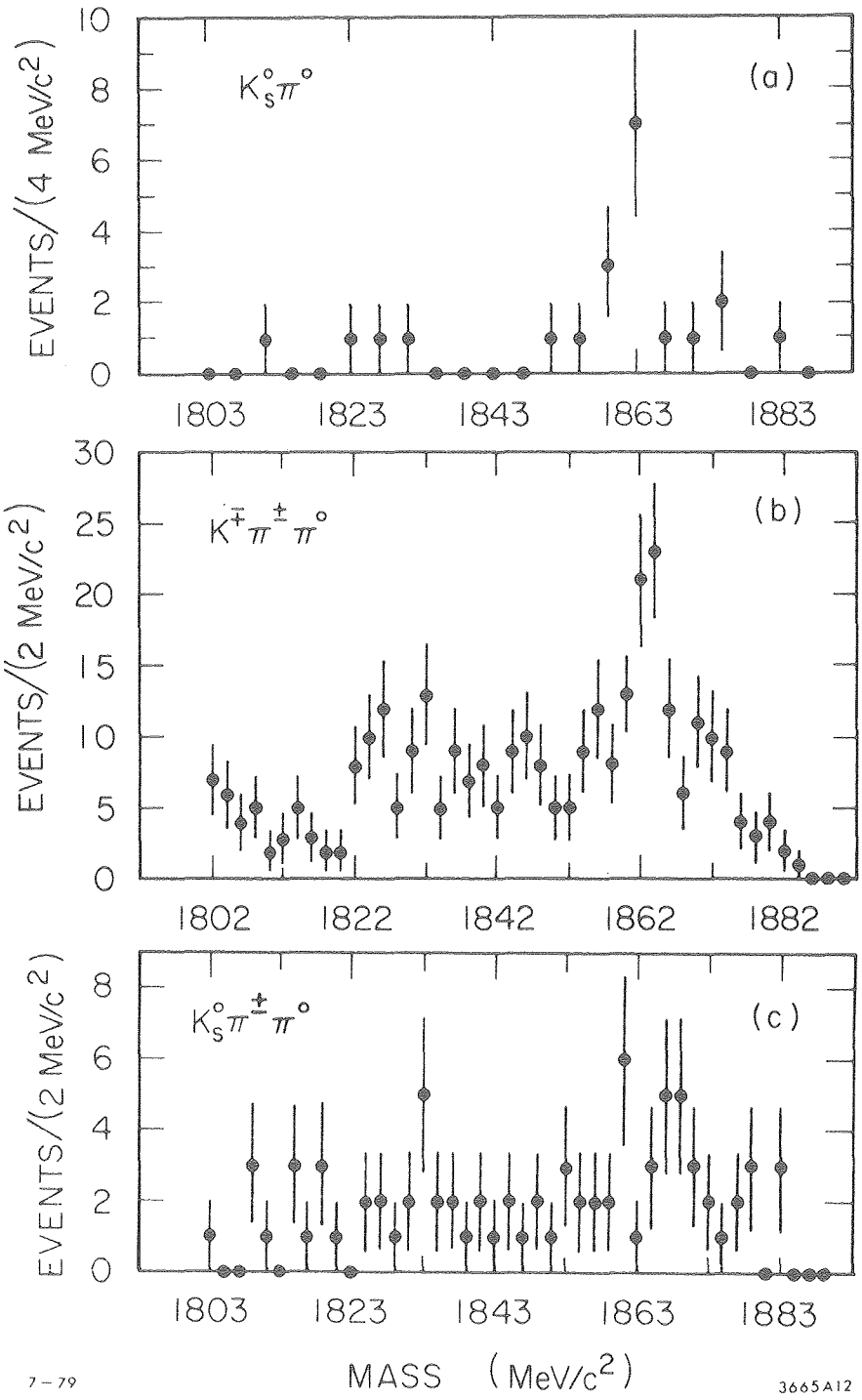

XBL 801-7868

Figure 4.5. Several D beam-energy-constrained mass distributions for decays involving π^0's obtained by the Mark II Collaboration at the ψ''.

a technique implicitly assumes D^0's and D^+'s are pair produced at the ψ'' and hence have exactly half the total center-of-mass energy. In the spirit of this assumption, some background is eliminated by only histograming events with a detector-measured energy within 50 MeV of the beam energy. Use of the beam-constrained mass offers unparalleled resolution and background rejection.

Fits to the signals shown in the above figures have been used to determine σBr and Br for various decay modes. This information is summarized in Table 4.2.

CABIBBO-SUPPRESSED DECAY MODES. An intrinsic part of the GIM mechanism for charm is the prediction that in addition to the principal (Cabibbo-favored) D decay modes, which lead to K^- or $\bar{K}^0$ in the final states, there are also Cabibbo-suppressed modes producing zero strangeness final states. The Cabibbo-favored and -suppressed modes for D^0 two-particle final states are illustratec by the quark diagrams in Fig. 4.6, where θ_A is the familiar Cabibbo angle and θ_B is a new angle which in the four-quark model is associated with the flavor mixing of charmed quarks. The GIM assumption is that $\theta_A = \theta_B$. Experimentally one can independently measure these angles using:

$$\tan^2 \theta_A = \frac{\Gamma(D^0 \rightarrow K^- K^+)}{\Gamma(D^0 \rightarrow K^- \pi^+)} \quad \text{and} \quad \tan^2 \theta_B = \frac{\Gamma(D^0 \rightarrow \pi^- \pi^+)}{\Gamma(D^0 \rightarrow K^- \pi^+)} .$$

The above expressions neglect the phase space corrections due to the K, π mass difference which will raise the $\pi^+\pi^-$ rate by 7% and lower the K^+K^- rate by 8%.

Figure 4.7 shows the Mark II $\pi^-\pi^+$, $K^-\pi^+$ and K^-K^+ invariant mass distributions for two-particle combinations with momentum within 30 MeV/c

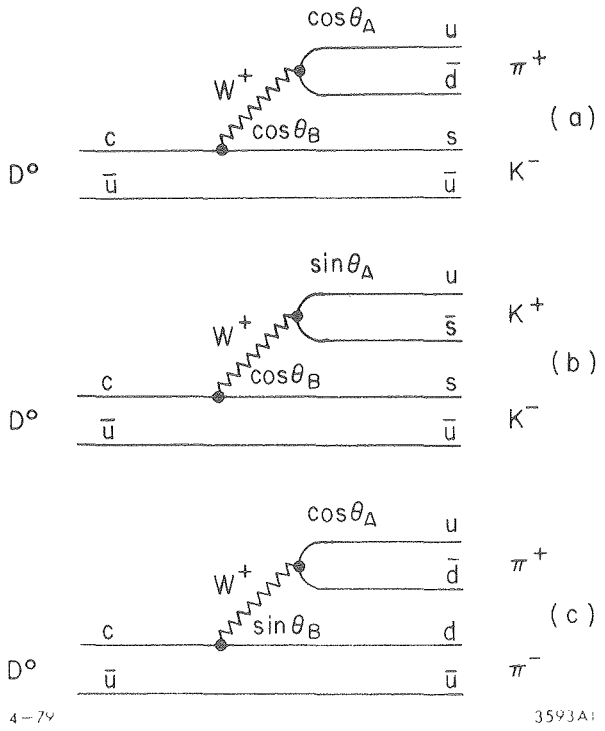

Figure 4.6. Quark diagrams for D^{o} decays into two charged particles.

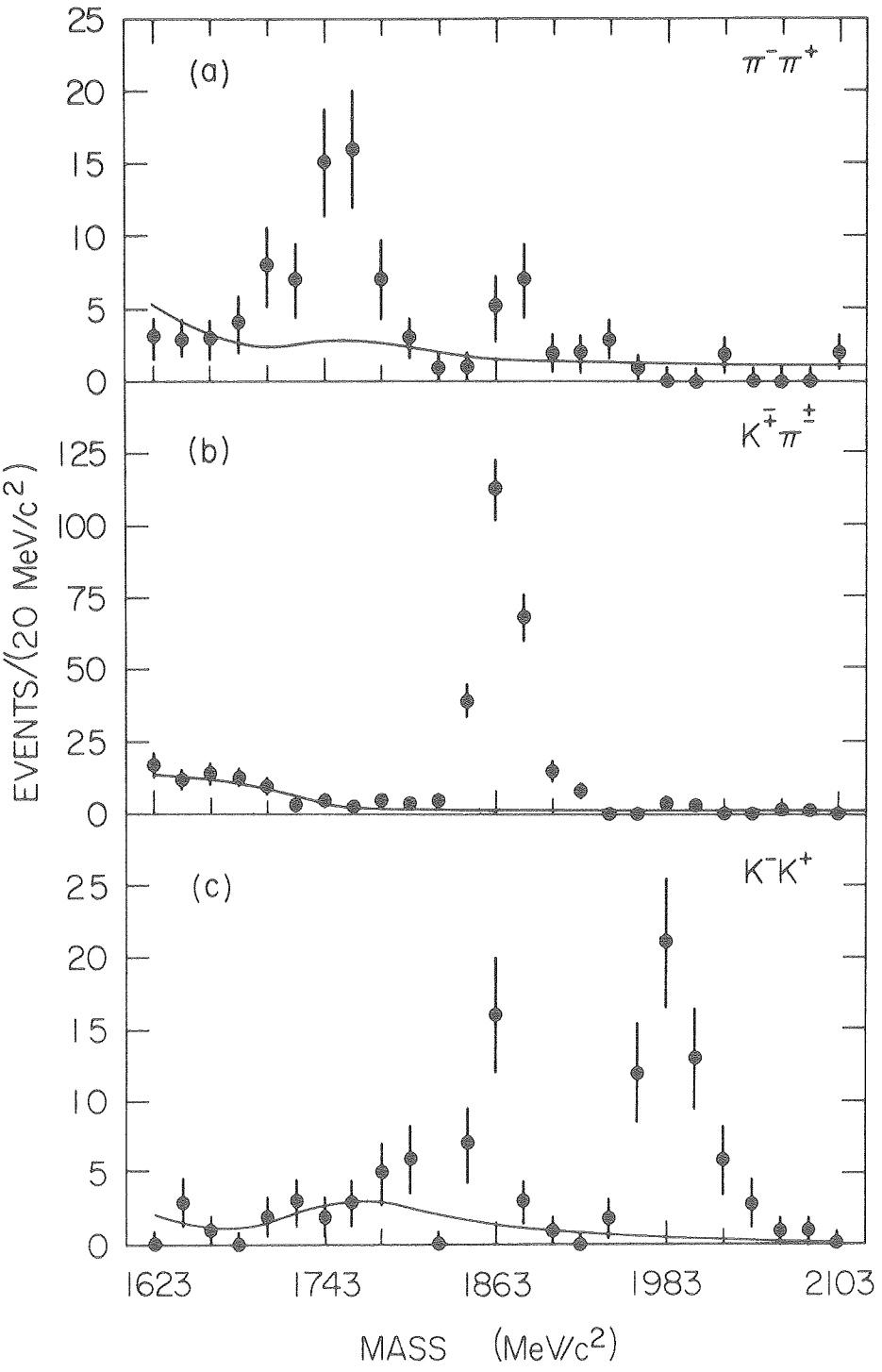

Figure 4.7. Evidence for two-body Cabibbo-suppressed decay modes obtained by the Mark II Collaboration at the ψ''. Candidates are required to have momenta within 30 MeV of that expected for D-pair production. Both figures (a) and (c) show prominent reflection peaks not centered at the D^o mass due to π/K misidentification by their time-of-flight system. The solid curves are background estimates.

of the expected D pair momentum at the ψ''. Aside from the signals in the three channels at the D mass one notes kinematic reflections shifted by about $\pm$ 120 MeV/c^2 from the D mass due to $\pi \leftrightarrow K$ misidentifications. A fit to the data yields 235 ± 16 $K^{\mp}\pi^{\pm}$ events, 22 ± 5 K^+K^- events and 9 ± 3.9 $\pi^+\pi^-$ events. After correcting for the relative efficiencies one obtains:

$$\frac{\Gamma(D^0 \rightarrow K^-K^+)}{\Gamma(D^0 \rightarrow K^-\pi^+)} = 0.113 \pm 0.03 \qquad (4.2)$$

and

$$\frac{\Gamma(D^0 \rightarrow \pi^-\pi^+)}{\Gamma(D^0 \rightarrow K^-\pi^+)} = 0.033 \pm 0.015 \quad , \qquad (4.3)$$

where the quoted errors include systematic effects. The results clearly demonstrate the existence of the Cabibbo-suppressed decay modes of roughly the expected magnitude: $\tan^2\theta \simeq 0.05$, although the $\pi\pi$ ratio is lower by about one standard deviation and the KK ratio is higher by about two standard deviations.

We note that the discrepancy between Eq. (4.2) and the pre-charm measurements of the Cabibbo angle cannot be trivially explained by the presence of additional mixing angles in the Kobayashi-Maskawa model. Hence the discrepancy (if not statistical in origin) implies a violation of SU(3) invariance due to unknown dynamical effects. It is thus premature to use Eq. (4.3) as a measure of the "new" Cabibbo angle (Abrams 1979).

4.3. Semileptonic Decay Modes

The prompt leptons created in the semileptonic decay of charmed mesons have been used both to estimate the rate for hadronic charm production, as well as to trigger detectors looking for the decay of charmed

particles into exclusive hadronic final states. Because it is possible to theoretically estimate the D semileptonic width (i.e., $\Gamma(D \rightarrow Ke\nu)$), a measurement of the semileptonic branching ratio can be used to estimate the D lifetime. At the time of this writing, emulsion as well as precision bubble and streamer chamber studies are being performed which are able to observe D's traveling finite distances before decaying, directly measure their lifetimes, and thus check current theoretical ideas on D semileptonic decays (Voyvodic 1979).

Because D semileptonic decays produce a neutrino in the final state, their study in e^+e^- annihilation invariably requires the measurement of inclusive final state electron or muon rates at center-of-mass energies where charmed mesons are known to be copiously produced. Inclusive electrons rather than muons are generally studied since the charged lepton in $D \rightarrow \bar{K}e^+\nu$ or $D \rightarrow \bar{K}\mu^+\nu$ has a momentum spectrum which peaks near 500 MeV for D's produced near threshold. Hence muons would be produced with momenta too low to cleanly be separated from pions using conventional hadron filters.

THE AVERAGE SEMILEPTONIC BRANCHING RATIO. Several basic techniques for extracting the D semileptonic branching ratio have been discussed in the literature. The simplest method (experimentally) estimates the branching fraction $Br(D \rightarrow eX) \equiv \Gamma(D \rightarrow eX)/\Gamma(D \rightarrow \text{all})$ from the ratio of the total electron to the total charm meson inclusive cross section or:

$$Br(D \rightarrow eX) = \frac{\sigma(e^+e^- \rightarrow e^{\pm} + \text{hadrons})}{\sigma(e^+e^- \rightarrow DX)} \quad . \qquad (4.4)$$

This method, the first historically (Braunschweig 1976, Burmester 1976), continues to provide the best statistical information on the D

semileptonic branching ratio. It suffers from inevitable systematic problems however. In evaluating the numerator, one must be careful to exclude (or correct for) contributions from heavy lepton decays or electromagnetic processes. The most common way of minimizing this contamination is to demand that the electrons are accompanied by two or more charged hadrons. Since the τ heavy lepton is known to decay predominantly into final states containing leptons and single hadrons, the multihadronic backgrounds due to $e^+e^- \rightarrow \tau^+\tau^-$ production are expected to lie at about the 25% level (Perl 1980, Barbaro-Galtieri 1978) and can be subtracted using the measured τ branching fraction and computable production cross sections.

Several techniques, all subject to various systematic uncertainties, have been used to estimate the denominator of Eq. (4.4). Extraction of $\sigma(e^+e^- \rightarrow DX)$ is relatively straightforward at the ψ'' since, as discussed earlier, it is natural to assume that this resonance decays exclusively into D's via:

$$\begin{aligned} \psi'' &\rightarrow (56 \pm 3)\% \quad D^0\bar{D}^0 \\ &\rightarrow (44 \pm 3)\% \quad D^+D^- \quad . \end{aligned} \tag{4.5}$$

The fractions used in Eq. (4.5) follow from the assumption of equal D^0, D^+ production corrected for p-wave threshold factors. Since it is impossible to separate the semileptonic decays of the D^0 from those of the D^+ without using tagged events or measuring the dielectron rate as well as the single electron rate, one in effect measures a weighted average of the D^0, and D^+ semileptonic branching ratio with weights given by Eq. (4.5).

At center-of-mass energies above the ψ'' it is sometimes possible to extract $\sigma(e^+e^- \rightarrow DX)$ by counting hadronic D decays into exclusive

final states such as $D^0 \rightarrow K^-\pi^+$, $D^+ \rightarrow K^-\pi^+\pi^+$ and dividing by the hadronic branching ratios measured for these states at the ψ''. When this is not possible because of statistical limitations, or in data predating the ψ'', the D inclusive cross section can be estimated at a given center-of-mass energy via:

$$\sigma(e^+e^- \rightarrow DX) = (R - R_{old}) \times \sigma_{e^+e^- \rightarrow \mu^+\mu^-}$$

where R is the τ lepton corrected ratio of hadrons to μ pairs, and R_{old} is the value of R below the $\psi(3095)$, which presumably represents the cross-section contribution of the "old" u, d, and s quarks. Being cognizant of the possible contributions to both the numerator and denominator of Eq. (4.5) from other charmed objects such as the F^+ and charmed baryons, some authors refer to the semileptonic branching ratios obtained through this technique as the average "charm" semileptonic branching ratio rather than the D semileptonic branching ratio.

Table 4.3 summarizes the average semileptonic branching ratios derived through measurements of the single electron rate by various groups. Figures 4.8 - 4.10 give the average semileptonic branching ratio vs $E_{c.m.}$ for the DASP, LGW and DELCO data (note there is a factor of two difference between the quantities plotted in Fig. 4.10 and the other two). All data sets show a remarkable constancy in the value for the average branching ratio even though the relative contribution of the D^0, D^+, F^+, and Λ_c must be changing as a function of energy. At $E_{c.m.} = 4.028$ GeV, for example, measurements of exclusive final states show that $(70 \pm 10)\%$ of D's are neutral compared to the $(56 \pm 3)\%$ neutral D fraction assumed at the ψ'' (Rapidis 1979).

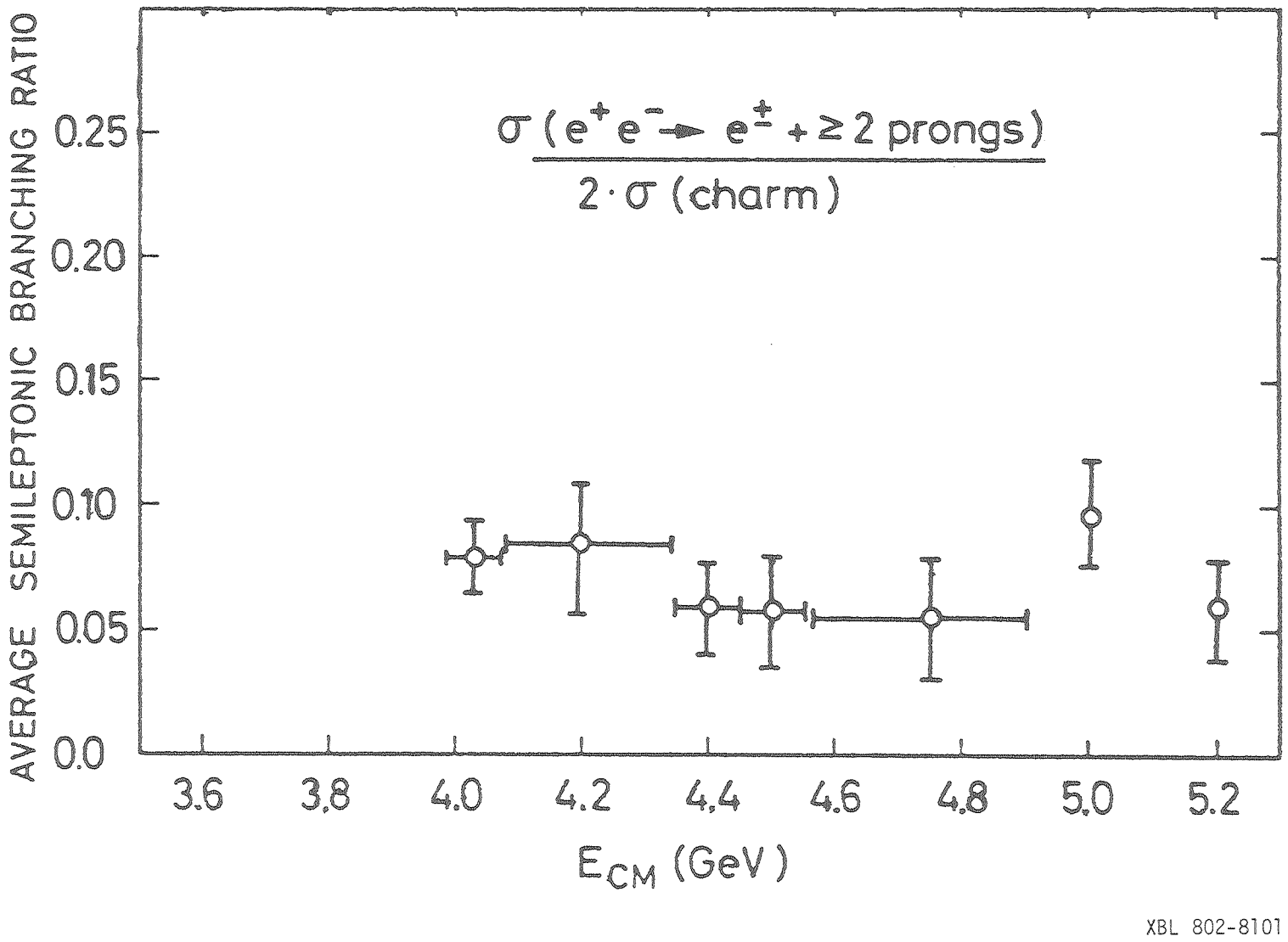

Figure 4.8. The average semileptonic branching ratio for charmed hadrons as a function of energy. The error bars are statistical only. DASP data.

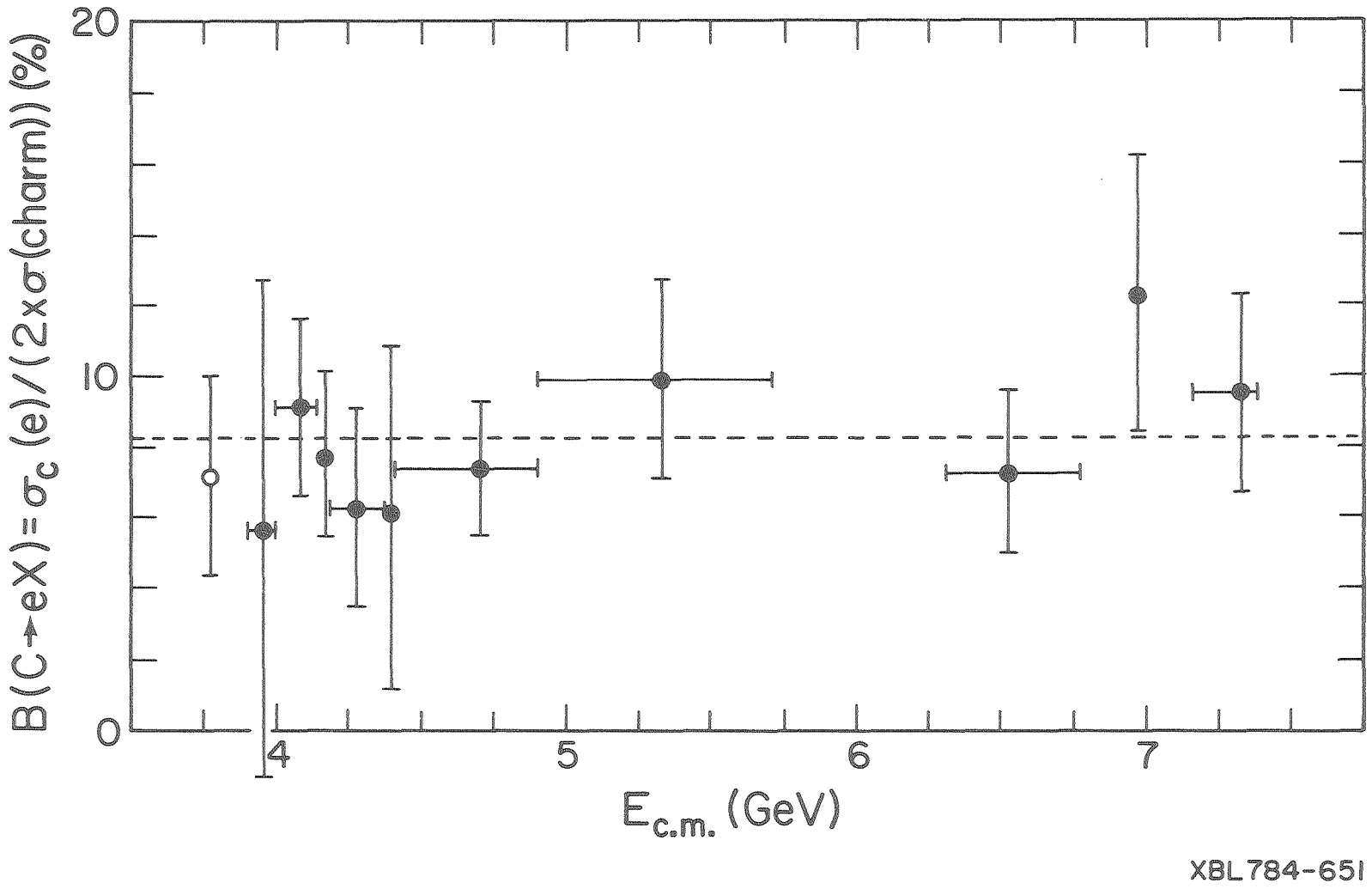

Figure 4.9. The branching fraction for charmed-particle decay into an electron plus additional particles as a function of energy (LGW collaboration). The dashed line indicates the average value of the ratio for $3.9 < E_{c.m.} < 7.4$ GeV.

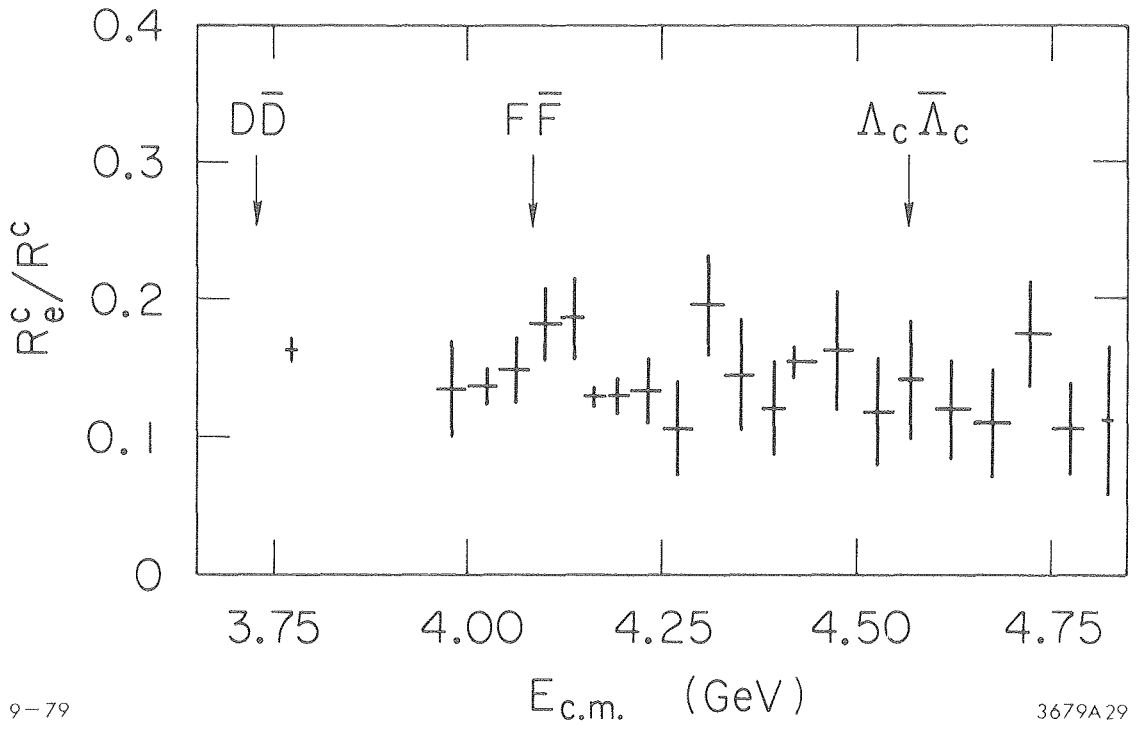

Figure 4.10. The ratio of R_e^c to the total charm hadronic cross section, R^c, measured by DELCO. The ratio R_e^c/R^c is equal to $2b_e(1-b_e)$, where the branching ratio, b_e = b(charm $\rightarrow$ eνX). (Kirkby 1979)

THE INCLUSIVE ELECTRON MOMENTUM SPECTRUM. Aside from studying the rate for charm-associated inclusive electron production, it is interesting to study the momentum distribution. Figures 4.11 show the inclusive momentum distribution obtained at the ψ'' by DELCO for events with ≥ 2 additional charmed particles. As the curves of the figure show, the momentum spectrum is consistent with the distribution expected for a mixture of $D \rightarrow Ke\nu$, $K\pi e\nu$, and $\pi e\nu$ semileptonic decays. The $Ke\nu$ and $K\pi e\nu$ contributions dominate over the Cabibbo-suppressed $\pi e\nu$ mode and appear to be roughly equal. The exact ratio of $K\pi e\nu$ to $Ke\nu$ depends sensitively on how much of the $K\pi$ is resonant as the $K^*(890)$.

TAGGED EVENTS. A second, potentially much cleaner technique for extracting the D semileptonic branching ratio involves counting the number of events containing an electron recoiling against a "tagging" $D^o \rightarrow K^-\pi^+$, $K^-\pi^+\pi^+\pi^-$ or $D^+ \rightarrow K^-\pi^+\pi^+$ candidate produced at the ψ''. Because the ψ'' cannot decay into final states containing a D^*, one is guaranteed that D^-'s are always produced against tagged D^+'s and $\bar{D}^o$ are always produced against tagged D^o's. Hence the tagging technique allows one to separately measure the D^+ and D^o semileptonic branching ratio. Owing to the smallness of tagging branching ratios, however, the number of tagged electron events is much smaller than the number of inclusive electron events, and such studies suffer from larger statistical errors.

Table 4.4 summarizes the Mark II collaboration's information on the D^o and D^+ semileptonic branching ratio (Lüth 1979). Wrong-sign e-tag events were used to compute the background level due to an $\simeq 6\%$ π/e misidentification. We see from Table 4.4 that the D^o and D^+ semileptonic branching ratio are unequal at about the two standard deviation level.

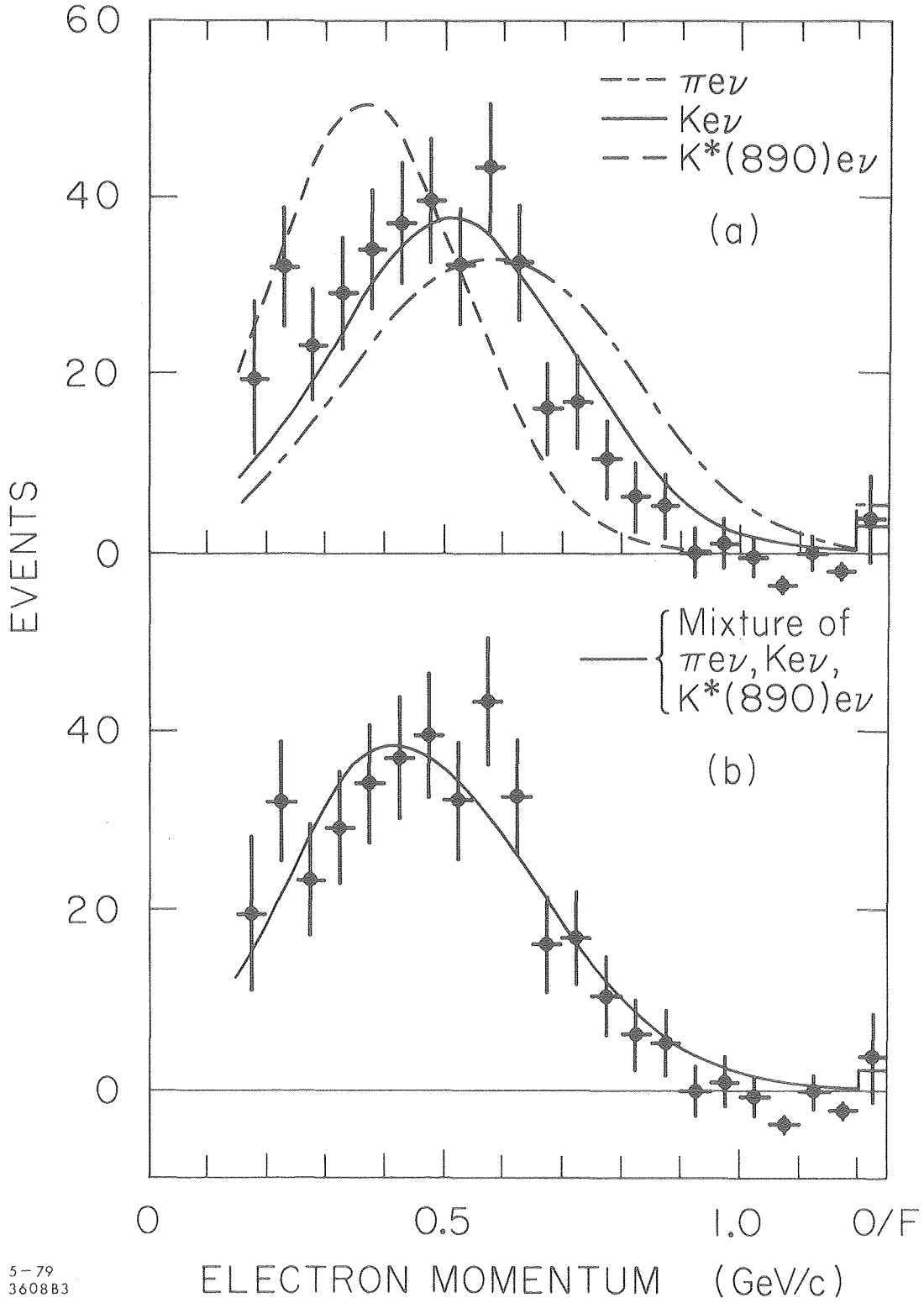

Figure 4.11. The electron momentum spectrum from D decays at the ψ", measured by DELCO. The curves have been fitted to the data below 1 GeV/c and correspond to the following hypotheses: (a) $D \rightarrow \pi e\nu$ (dot-dashed curve, $\chi^2/dof = 80.9/16$), $D \rightarrow Ke\nu$ (solid curve, $\chi^2/dof = 23.4/16$), $D \rightarrow K^*(890)e\nu$ (dashed curve, $\chi^2/dof = 53.8/16$). (b) Contributions from $D \rightarrow Ke\nu$ (55%), $D \rightarrow K^*e\nu$ (39%) and $D \rightarrow \pi e\nu$ (6%) with $\chi^2/dof = 11.2/15$ (Kirkby 1979).

We should also mention that the use of tagged events at the ψ'' has provided important information on the kaon content of D decays, and the D decay final state multiplicity distribution (Feller 1979, Schindler 1979, Lüth 1979, Vuillemin 1978).

TWO-ELECTRON FINAL STATES. This conclusion is corroborated by the DELCO collaboration's analysis of the two-electron versus one-electron rate at the ψ'' (Kirkby 1979). In the limit of perfect acceptance, the single (N_1) and double (N_2) electron event rates due to D decays are related to the neutral (b_o) and charged (b_+) semileptonic branching ratios by

$$\begin{aligned} N_1 &= 2N_o b_o(1 - b_o) + 2N_+ b_+(1 - b_+) \\ N_2 &= N_o b_o^2 + N_+ b_+^2 \end{aligned} \tag{4.6}$$

where N_o and N_+ are the number of D^{o-o} and D^+D^- events produced. One sees from Eq. (4.6) that in the limit of small branching ratios a measurement of N_1 deterimines essentially a line in the b_o vs b_+ plane whereas a measurement of N_2 determines an elliptical arc. One thus expects that a simultaneous measurement of N_2 and N_1 will lead to two ambiguous solutions for b_o and b_+. Figure 4.12 indicates the experimental regions in the b_+ vs b_o plane which are consistent to within one standard deviation with the data presented in Table 4.5. The data has been corrected for electron detection efficiency using the two extreme models that $D \to Ke\nu$ (Fig. 4.12(a)) or $D \to K^*e\nu$ (Fig. 4.12(b)). Under either assumption it appears that $b_o \gg b_+$ or $b_+ \gg b_o$. DELCO uses the K_S content in the two-electron events to distinguish between these two possibilities. Although both D^o's and D^+'s can decay into K_S, the D^o must do so via the decay sequence $D^o \to (K\pi)^- e^+ \nu$ where the isodoublet $K\pi$ system decays

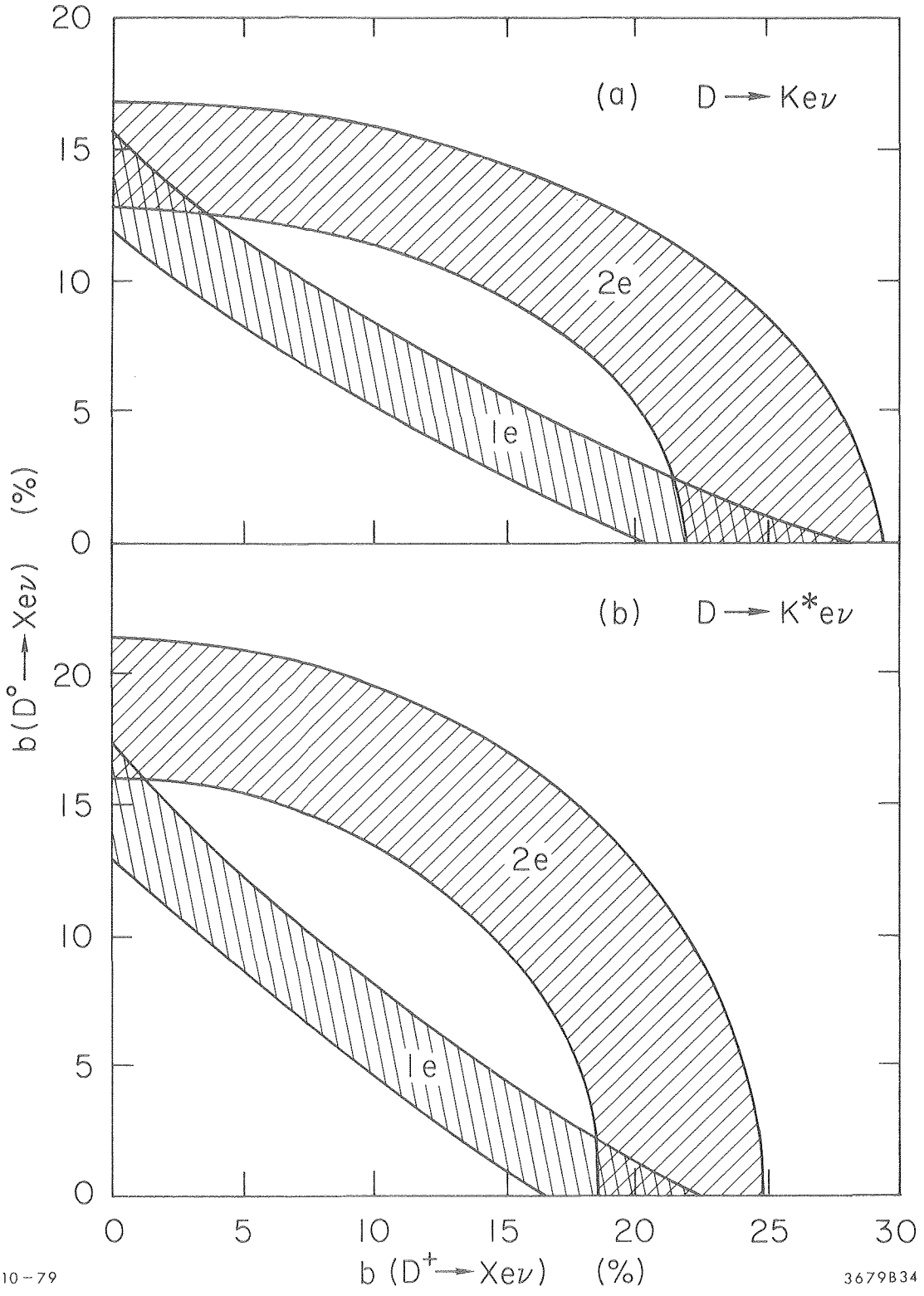

Figure 4.12. The allowed solutions for the D^{o} and D^{+} semileptonic branching ratios in the DELCO 1e and 2e multiprong data at the ψ''. The shaded regions, which correspond to $\pm 1\sigma$ limits, are plotted for two extreme assumptions of the detection efficiencies: (a) all $D \rightarrow Ke\nu$ and (b) all $D \rightarrow K^{*}e\nu$ (Kirkby 1979).

into a charged kaon 2/3 of the time ($I = 1/2$) and a neutral kaon only 1/3 of the time. The D^+, on the other hand, can produce K_S via both $D^+ \to K_S e^+ \nu$ and $K_S \pi^o e^+ \nu$. In fact a rather large fraction of the two-electron events (8 out of 16.4) have a K_S which suggests the solution $b_+ \gg b_o$. Combining the information on the single-electron and two-electron rate at the ψ'' with the K_S content of the two-electron events, DELCO finds the D^+ and D^o semileptonic branching ratios to be $(24 \pm 4)\%$ and $< 5\%$ (95% C.L.) respectively, in agreement with the trend and values of the Mark II data.

THE D^o, D^+ LIFETIMES. Because of the isosinglet character of the Lagrangian responsible for the Cabibbo-favored D semileptonic decay one expects that $\Gamma(D^+ \to K m\pi e^+ \nu) = \Gamma(D^o \to K m\pi e^+ \nu)$ for any number m of pions (see for example Pais & Treiman 1977). Hence, neglecting the Cabibbo-suppressed decay modes one has the relation: $b_o \Gamma_o(D^o \to \text{all}) = b_+ \Gamma(D^+ \to \text{all}) = \Gamma(D \to KeX)$. In terms of lifetimes, one thus obtains $\tau(D^+)/\tau(D^o) > 4$ (95% C.L.) for the DELCO data, and $\tau(D^+)/\tau(D^o) = 3.1^{+4.1}_{-1.3}$ for the Mark II. One can estimate the order of magnitude of the D lifetime using the theoretical calculation for the $D \to Ke\nu$ width of about 10^{11} sec^{-1} (see for example Fakirov & Stech 1978) and the ratio $\Gamma(D \to Ke\nu)/\Gamma(D \to eX) = (45 \pm 24)\%$ obtained through the DELCO fit to the ψ'' electron momentum spectrum. These results suggest that the D^+ lifetime is on the order of 10^{-12} sec while the D^o is three to five times shorter lived.

Owing to the large phase space and number of hadronic decay modes available to both charmed mesons, it appears surprising that hadronic decays of the D^+ can be suppressed by at least a factor of three to five

relative to those of the D^o as suggested by the recent data. We note that the average charm semileptonic branching ratio reported by all groups appears to be remarkably constant as a function of center-of-mass energy. Within the limits of the present statistical and systematic uncertainties these measurements are not inconsistent with the observation of different lifetimes, however one should eventually be able to measure significant variations in the semileptonic branching ratio in data taken at different center-of-mass energies.

5. THE EXCITED STATES OF CHARM

5.1. Observation of $D^{*+} \rightarrow \pi^+ D^o$

Structure present in the early D meson recoil spectra obtained by the SLAC-LBL Mark I collaboration suggested the presence of D^*'s or heavier, new charmed mesons produced against the D in e^+e^- annihilation. Direct evidence for the D^{*+} was obtained by this group (Feldman 1977) in data collected from 5 to 7.8 GeV, the energy limit of SPEAR. In an effort to observe the pion cascade process $D^{*+} \rightarrow D^o\pi^+$, $D^o \rightarrow K^-\pi^+$ candidates with masses in the D region from 1.820 to 1.910 GeV and momenta exceeding 1.5 GeV were paired with extra pions of the appropriate charge. Figure 5.1 shows the resulting mass difference, $M(D^o\pi^+) - M(D^o)$, distribution. Relatively large momenta D^o's were required in order that the pions produced in the process $D^{*+} \rightarrow \pi^+ D^o$ had sufficient momenta to be observed in their detector.

A clear, nearly background-free signal is seen in the $D^o\pi^+$, $\bar{D}^o\pi^-$ distribution at a mass difference of 145.3 ± 0.5 MeV. The narrow width of this peak sets the limit $\Gamma_{D^{*+}} < 2$ MeV/c^2 (90% C.L.). The slight enhancement at the same mass difference for $D^o\pi^- + \bar{D}^o\pi^+$ events can

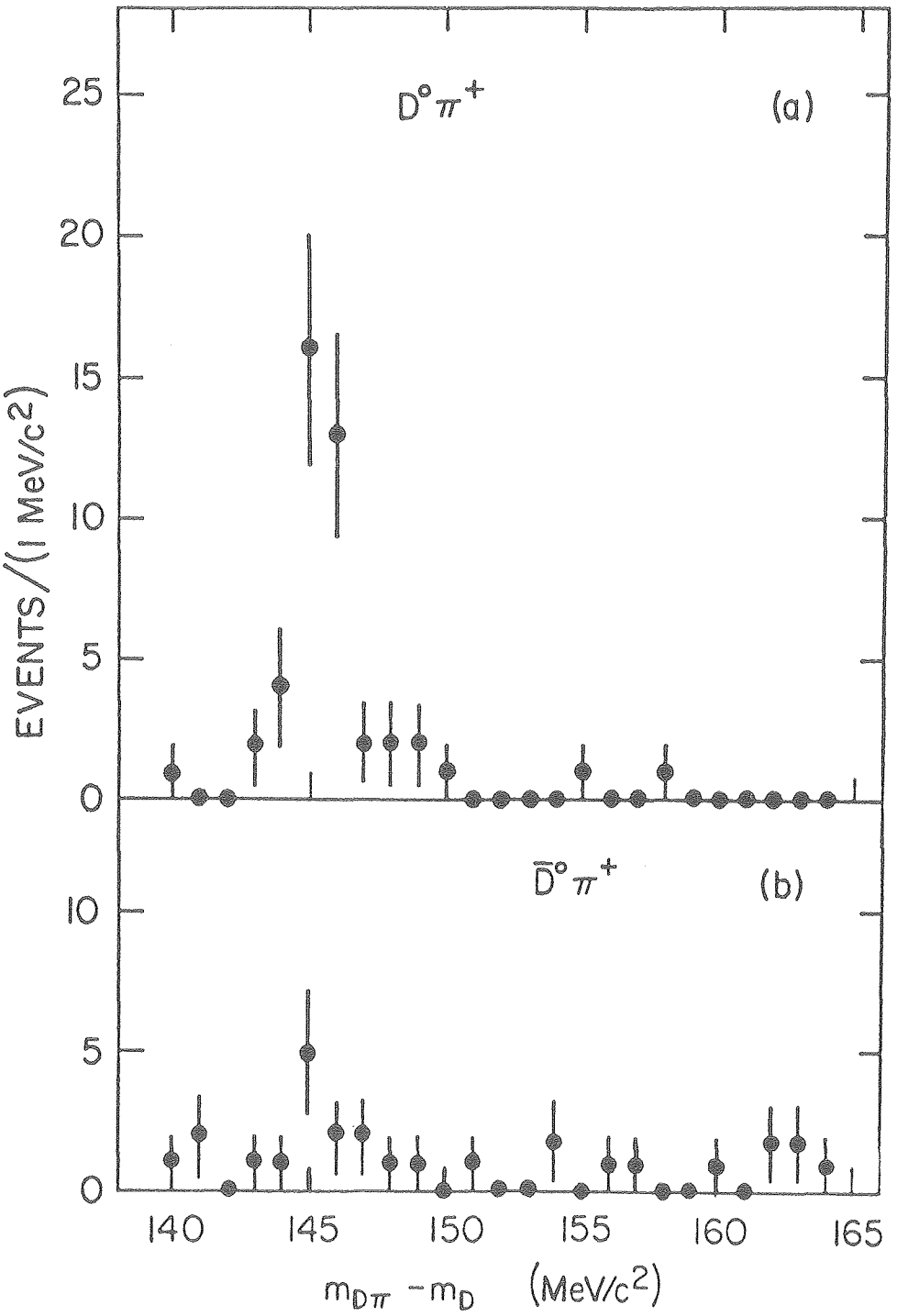

Figure 5.1. The $D^\circ\pi^+$ (a) and $\bar{D}^\circ\pi^+$ (b) mass difference distributions for $D^\circ \to K^-\pi^+$ candidates lying within 45 MeV of the D° mass obtained by the Mark I collaboration. The slight signal in (b) is consistent with that expected from double time-of-flight misidentification. The charge conjugate reactions are included.

be explained by π/K misidentification by the time-of-flight system. The relative smallness of this peak compared to the peak of Fig. 5.1(a) sets a limit on the conjectured $D^0 - \bar{D}^0$ mixing process that less than 16% of produced D^0's mix into $\bar{D}^0$'s within the D^0 lifetime. Finally it was found that a substantial (i.e., $25 \pm 9\%$) fraction of D^0's produced in their data sample with momenta exceeding 1.5 GeV are from the D^{*+} pionic decay.

5.2. Evidence for the D^{*0}

A natural extrapolation of this D^{*+} observation is that there exists an excited state of the D^0, as well. Thus one would have an excited (D^{*0}, D^{*+}) isodoublet which might, for example, be a spin excitation of the (D^0, D^+) system. Figure 5.2(a), which shows the recoil mass distribution against $D^0 \to K^-\pi^+$ candidates collected at a center-of-mass energy of 4.028 GeV, provides evidence for the existence of the D^{*0} (Goldhaber 1977). This distribution has background $K^{\mp}\pi^{\pm}$ combinations with masses straddling the D^0 signal subtracted out. The two peaks present in Fig. 5.2(a) are attributed to the process $e^+e^- \to D^*\bar{D}$ or $\bar{D}^*D$, which produces a peak near 2.01 GeV, and $e^+e^- \to D^*\bar{D}^*$; $D^* \to \pi^0 D^0$, which produces a narrow reflection peak near 2.15 GeV. We note the relative smallness of the reaction $e^+e^- \to D\bar{D}$ which would produce a peak near 1.863 GeV.

The narrowness of the reflection peak near 2.15 GeV must follow from the small Q value for the pionic cascade process as well as the improved recoil mass resolution for D^*'s produced nearly at threshold. This small Q value allows the radiative D^* decay process, $D^{*0} \to \gamma D^0$, to compete favorably with the pionic cascade as we shall demonstrate

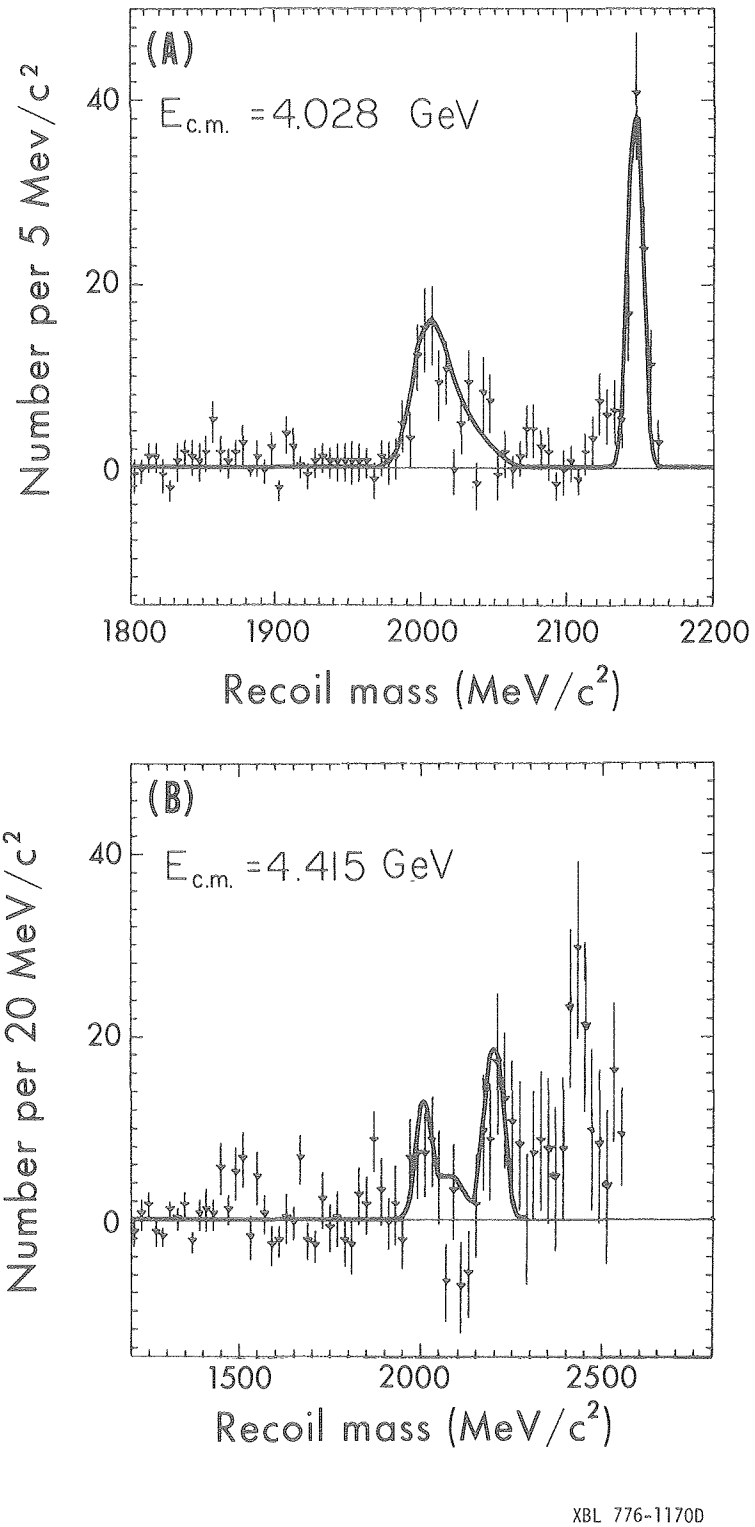

Figure 5.2. The D^{o}-subtracted recoil spectra obtained by the Mark I collaboration at two fixed energies. Please note the scale changes.

later. Processes such as $e^+e^- \to \bar{D}_1^o$, D^{*o}; $D^{*o} \to D_2^o\pi^o$ where D_2^o rather than D_1^o is observed decaying into $K^-\pi^+$ give rise to the trailing tail of the peak near 2.15 GeV.

The solid curves superimposed on Fig. 5.2(a) give the expected shapes for the $D^*\bar{D}$ and $D^*\bar{D}^*$ contributions to the D^o recoil spectrum at $E_{c.m.} = 4.028$ GeV. These curves neglect any $D^* \to \gamma D$ contributions, however. Figure 5.2(b) shows the D^o spectrum obtained for data collected at $E_{c.m.} = 4.415$ GeV overplotted with the expected shape of contributions from these same two processes.

Comparison of the second peak in Figs. 5.2(a) and 5.2(b) show that this peak moves and broadens in the manner expected for a kinematic reflection. The origin of the peak near 2.44 GeV in the $E_{c.m.} = 4.415$ GeV is as yet unclear -- it may be due to multibody final states such as $D^{*o}\bar{D}^{*o}\pi^o$ or possible evidence for a D^{**}.

5.3. The Masses and Branching Ratios of the D^*'s

In order to quantitatively analyze D production at $E_{c.m.} = 4.028$, a fit was performed to the joint D^o and D^+ momenta spectra. Owing to the kinematic simplicity of the symmetric annihilation process, the D momentum can be trivially related to the value of the recoil mass against the D. The momentum variable does, however, offer the advantage that the D momentum resolution is a relatively insensitive function of momentum near threshold. The decay mode $D^{*+} \to \pi^+D^o$ couples the charged and neutral D momentum spectra, thus necessitating a single fit to both.

Figure 5.3(a) illustrates eight contributions to the D^o momentum spectrum at $E_{c.m.} = 4.028$ GeV in terms of the three basic processes:

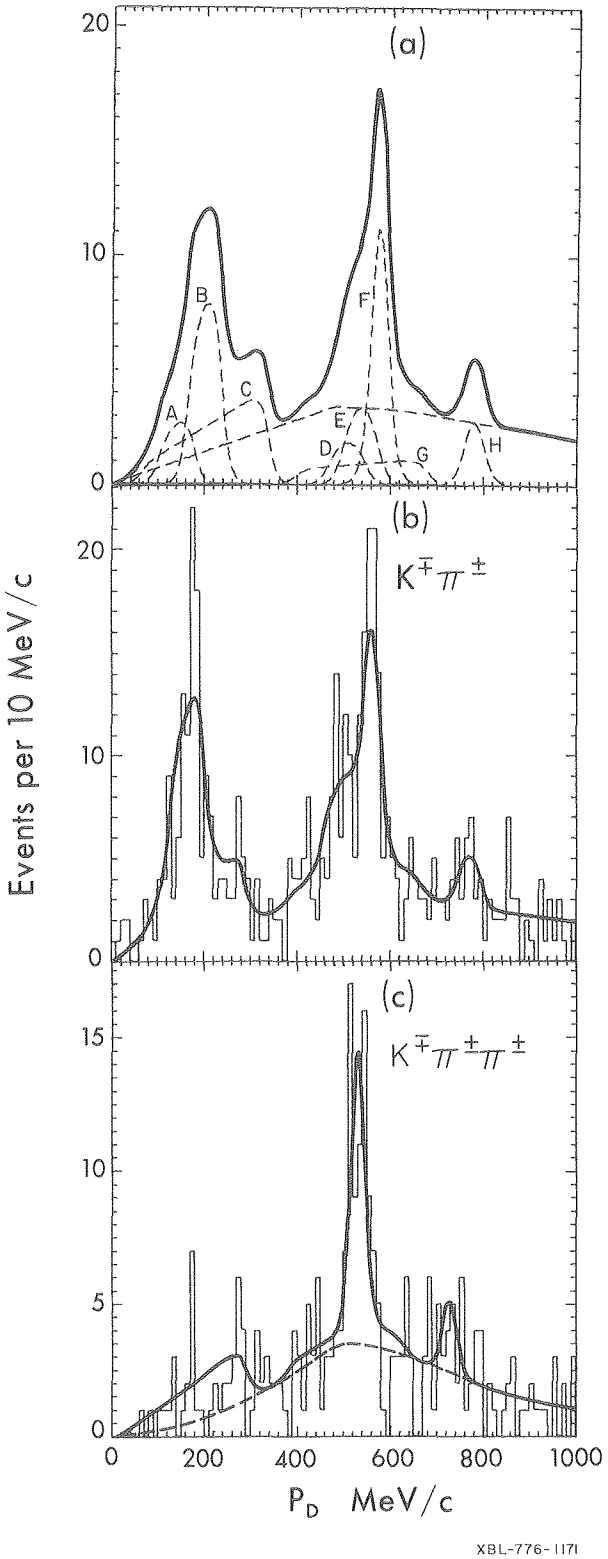

Fig. 5.3. The D momentum spectrum at 4.03 GeV from Goldhaber (1977). (a) Contribution to the expected D^o momentum spectrum from:

A: $e^+e^- \rightarrow D^{*+}D^{*-}$, $D^{*+} \rightarrow \pi^+ D^o$

B: $\rightarrow D^{*o}\bar{D}^{*o}$, $D^{*o} \rightarrow \pi^o D^o$

C: $\rightarrow D^{*o}\bar{D}^{*o}$, $D^{*o} \rightarrow \gamma D^o$

D: $\rightarrow D^{*+}D^-$, $D^{*+} \rightarrow \pi^+ D^o$

E: $\rightarrow D^{*o}\bar{D}^o$, $D^{*o} \rightarrow \pi^o D^o$

F: $\rightarrow \bar{D}^{*o}D^o$, direct D^o

G: $\rightarrow D^{*o}\bar{D}^o$, $D^{*o} \rightarrow \gamma D^o$

H: $\rightarrow D^o\bar{D}^o$, direct D^o

(b) $D^o \rightarrow K^-\pi^+$ momentum spectrum, the curve is the result of the fit and (c) $D^+ \rightarrow K^-\pi^+\pi^+$ momentum spectrum where the curve is the result of the fit and the dashed line is the background.

(i) $e^+e^- \rightarrow D\bar{D}$

(ii) $e^+e^- \rightarrow D\bar{D}^* + \bar{D}D^*$

(iii) $e^+e^- \rightarrow D^*\bar{D}^*$

where D^*'s decay ultimately into D's via the reactions:

(iv) $D^{*+} \rightarrow \pi^+ D^o$

(v) $D^{*+} \rightarrow \pi^o D^+$

(vi) $D^{*+} \rightarrow \gamma D^+$

(vii) $D^{*o} \rightarrow \pi^o D^o$

(viii) $D^{*o} \rightarrow \gamma D^o$

The fit does indeed show that D production at this energy is overwhelmingly dominated by the two-body processes (i) through (iii). Less than 10% of the D^o's were found to arise from the three-body process $D^o\bar{D}^o\pi^o$. The positions and shapes of these contributions depend sensitively on the D^* masses and $D^* - D$ mass differences. The relative areas of these contributions are functions of the rates for processes (i), (ii) and (iii) and the various D^* branching ratios.

Table 5.1, reprinted from Goldhaber (1977), summarizes the information obtained from two fits to the joint $D^o \rightarrow K^-\pi^+$, and $D^+ \rightarrow K^-\pi^+\pi^+$ momentum spectra. The detailed assumptions for both fits are described in this reference, but a few words are in order. Both fits embody the constraint $M_{D^{*+}} - M_{D^o} = 145.2$ MeV/c^2. The "normal" fit treats the two D^{*+} contributions to the D^o spectrum (via process (iv)) as independent parameters, whereas the "isospin-constrained" fit relates the number of D^o arising from $D^{*+}D^{*-}$ production to that from $D^{*+}D^-$ production via a universal $D^{*+} \rightarrow \pi^+ D^o$ branching ratio and the assumption that apart from p^3 threshold factors, the rates for the charged versions of processes

(i - iii) equal the rates for the neutral versions.

Both fits match the experimental momentum spectra reasonably well. In addition, the D masses and ratio of D^+/D^o branching fractions obtained in this fit agrees well with the results of later work by the LGW and Mark II collaborations obtained at the ψ''. These results are compared in Table 5.2. Figure 5.4 summarizes the mass relationships between the D and D^* systems.

We see from Table 5.1 that D^o production at $E_{c.m.} = 4.028$ GeV is dominated by nearly equal contributions from Reactions (ii) and (iii). This is notable in light of the 16-MeV Q-value for Reaction (iii) compared to a Q of 159 MeV and 312 MeV for reactions (ii) and (i) respectively. One expects some enhancement of Reaction (iii) due to the larger number of available final state spins but the spin factor is considerably smaller than the enhancement implied by the data when corrected by the expected p^3 threshold factors.

5.4. Spins of the D, D^* Mesons

Because the D and D^* are the two lightest charmed particles, it is a priori probable that the D is a pseudoscalar residing in the SU(4) multiplet of the pion, while the heavier D^* is a vector residing in the SU(4) multiplet of the $\rho(770)$. Because of the large mass splitting within these SU(4) multiplets, and the presumably reduced strength of the quark hyperfine splitting for states containing a charmed quark, these conclusions may not hold. Present data is insufficient to establish the unique spin-parity assignments of the low-lying charmed mesons, although there is experimental information from SPEAR.

Some information is available from the study of the D^* decay modes

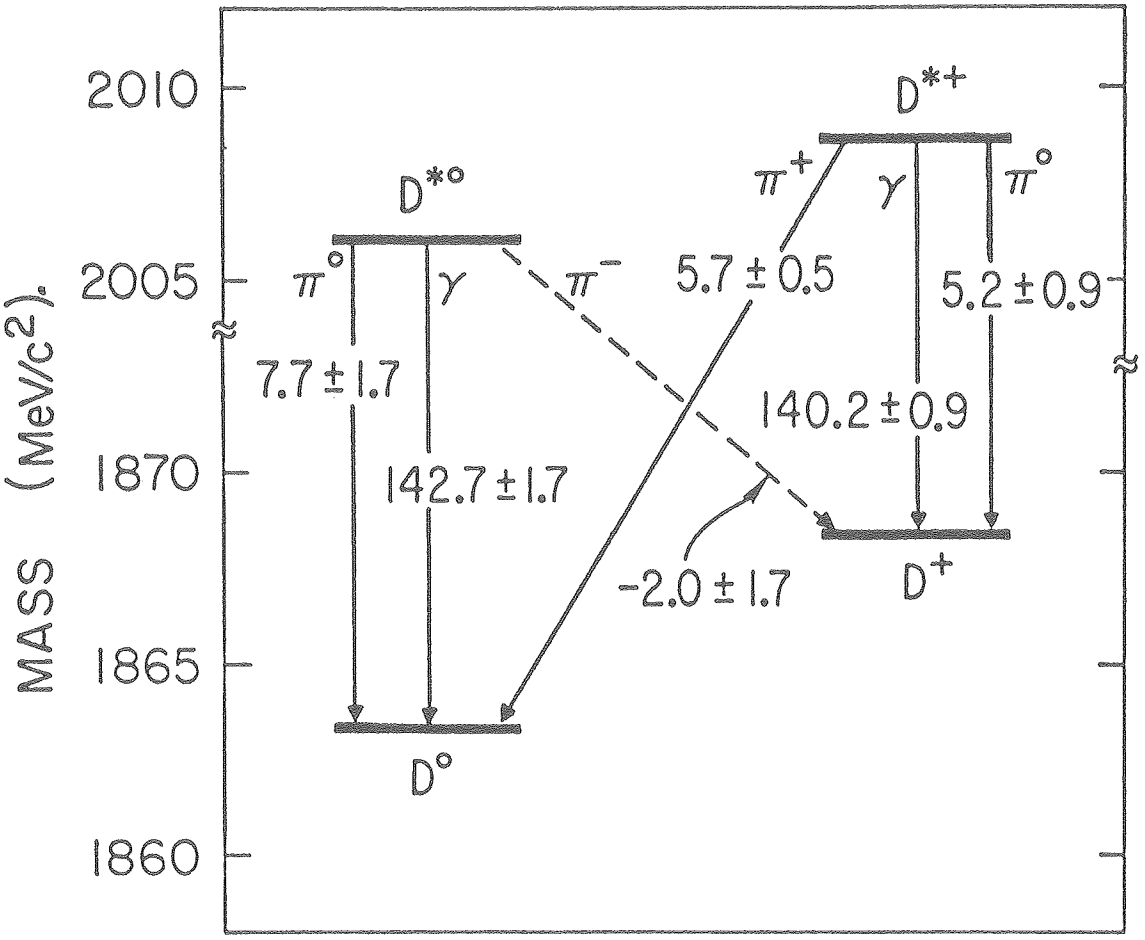

Figure 5.4. Mass level diagram giving the best current values for D^* and D states. The arrows represent different decay modes of the D^*; the numbers across the lines represent the Q for each decay expressed in MeV. The decay $D^{*o} \rightarrow D^+\pi^-$ is kinematically forbidden. The masses are (D^o) 1863.3 ± 0.9, (D^+) 1868.3 ± 0.9, (D^{*o}) 2006.0 ± 1.5 and (D^{*+}) 2008.6 ± 1.0 MeV/c^2.

discussed earlier. Observation of the decay $D^* \to \pi D$ along with the reaction $e^+e^- \to D\bar{D}^*$ demonstrates that the D and D^* are not both spinless.[1] Evidence for the radiative decay $D^* \to \gamma D$ corroborates this conclusion.

The LGW collaboration (Peruzzi 1977) has obtained information on the angular distribution (in θ) of the D momentum vector with respect to the e^+e^- annihilation axis for the reaction $e^+e^- \to D\bar{D}$ obtained in data collected at the ψ''. Figure 5.5 shows the background-subtracted cos θ distributions for $D^o(\bar{D}^o) \to K^{\mp}\pi^{\pm}$ and $D^{\pm} \to K^{\mp}\pi^{\pm}\pi^{\mp}$ events. Fits of these distributions to the form

$$\frac{dn}{d\ \cos\ \theta} \propto 1 + \alpha \cos^2 \theta$$

yields the values $\alpha = -1.04 \pm 0.10$ for the $D^{\pm}$ and $\alpha = -1.00 \pm 0.09$ for the $D^o(\bar{D}^o)$, which are remarkably close to the value $\alpha = -1$ required for production of spinless particles. Their result suggests that the D is spinless as expected; however two D's of higher spin could couple fortuitously to give a $\sin^2\theta$ polar distribution as well.

Spin information on the D and D^* is available from SLAC-LBL collaboration data on D's produced in e^+e^- annihilations at a center-of-mass energy of 4.028 GeV. At this energy D^o's are primarily produced via the processes $e^+e^- \to D^*\bar{D}^*$ and $D\bar{D}^*$. One can obtain a relatively pure sample of D's from either process by applying an appropriate cut on the measured recoil mass against the D^o.

The distribution for the angle between the D^* momentum and the annihilation axis, obtained for $D^*\bar{D}^*$ production, was fit to the form:

---

[1] If the D and D^* were both spinless they would require even relative parity to couple to a photon via $e^+e^- \to DD^*$. However then the decay $D^* \to \pi D$ would fail to conserve parity.

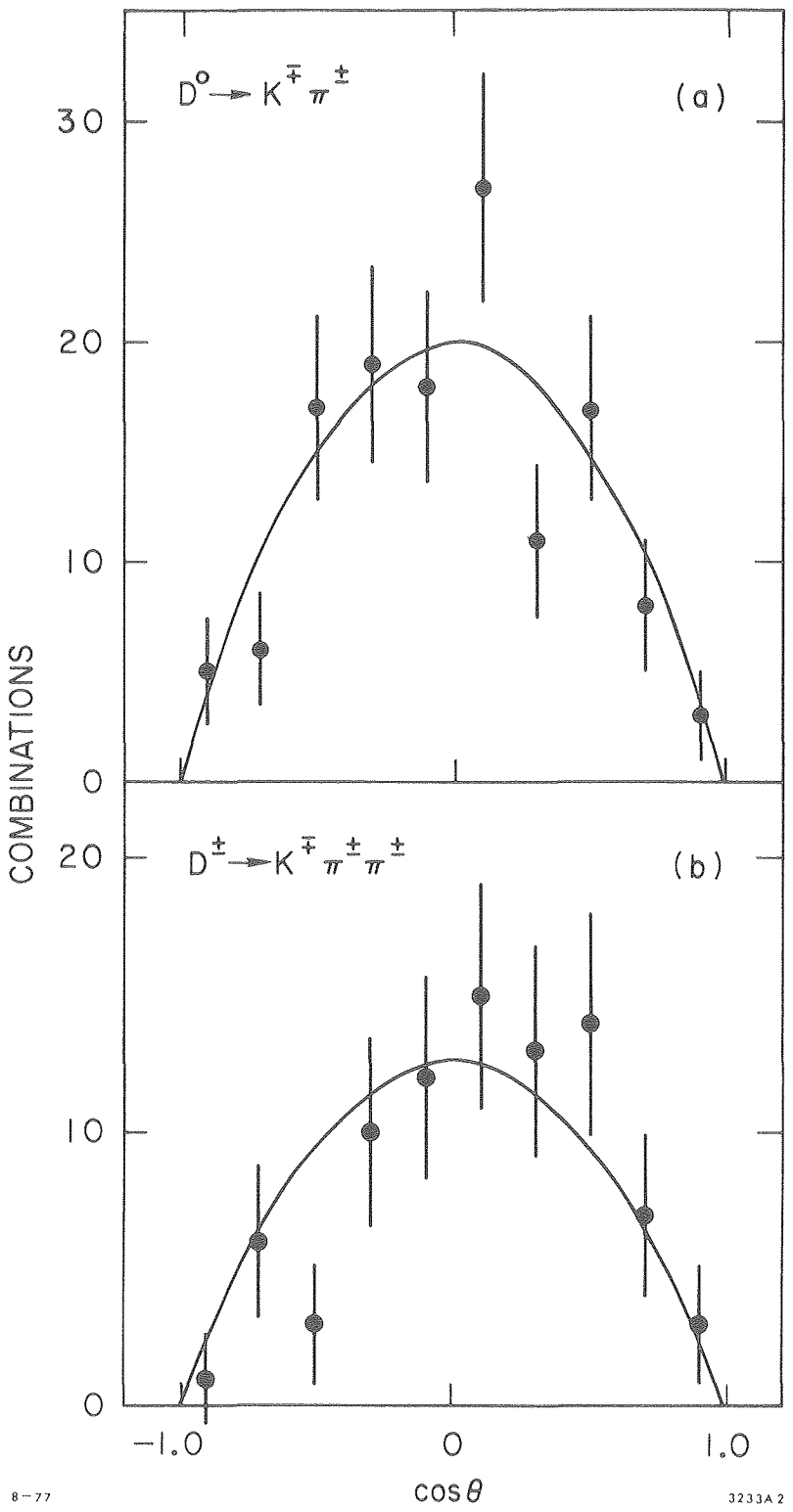

Figure 5.5. Cosine of the angle between the incident e^+ beam and the D momentum for (a) $D^0(\bar{D}^0) \to K^{\mp}\pi^{\pm}$ and (b) $D^{\pm} \to K^{\mp}\pi^{\pm}\pi^{\pm}$, after background subtraction. The curves represent $\sin^2\theta$, the required distribution for the production of spinless D mesons.

$$\frac{dn}{d\cos\theta} \propto 1 + \alpha \cos^2\theta \quad .$$

The measured value $\alpha = -0.3 \pm 0.3$ tends to rule out spinless D^*'s at the two-standard-deviation level.

A study of the joint production and decay angular distribution for the process $e^+e^- \rightarrow \bar{D}^*D^o$, $D^o \rightarrow K^-\pi^+$ provides additional information on the charmed meson spins. One can uniquely predict this distribution for the case of spin-0 D and spin-1 D^* and vice versa if one assumes that the two mesons have even relative parity (as evidenced under these spin assignments by the observation of the reaction $D^* \rightarrow \pi D$). In particular there would be a considerable anisotropy in the $D^o \rightarrow K\pi$ decay if a vector D^o was produced against a pseudoscalar D^*. Such an anisotropy is inconsistent with the SLAC-LBL data at about the three-standard-deviation level. Their data is fully consistent with the expected distribution for a pseudoscalar D and vector D^*, however (Nguyen 1977).

In summary, all known data on charmed meson spin is consistent with the expected vector character of the D^* and pseudoscalar character of the D. The two mesons cannot both be spinless, and the case of vector D's and pseudoscalar D^*'s is explicitly excluded. Nothing as of yet is known about the possibilities where the sum of the D and D^* spins exceeds one.

6. THE F MESON

Little is known experimentally about the third charmed meson -- the F^+. This isosinglet meson is constructed from a c and $\bar{s}$ quark and should decay predominantly into final states of zero strangeness according to

the GIM model. Since the many possible multipion F^+ decay modes are expected to have huge backgrounds, investigators have tended to search for F^+ decaying into less common particles such as $K^+K^-\pi^+$, K^+K_S, or η multipions.

At the time of this writing the only published observation of the F^+ comes from the DASP collaboration (Brandelik 1979) who look for the process $e^+e^- \rightarrow F\bar{F}^*$ where the $F \rightarrow \pi\eta$ and $\bar{F}^* \rightarrow \gamma\bar{F}$ (the $F^* \rightarrow \pi F$ decay does not conserve isospin).

Figure 6.1 shows the $\gamma\gamma$ invariant mass distribution for hadronic events collected at the indicated center-of-mass energies. The most pronounced η signal occurs near $E_{c.m.} = 4.42$, which is at the location of a 33-MeV wide resonance in R. Requiring the presence of an additional soft γ ($E_\gamma < 140$ MeV) in the event, as would be the case for F^*F or F^*F^* production, appears to enhance the η signal relative to the background in the 4.42-GeV data (see Fig. 6.2). These observations are thus suggestive of a substantial F^* contribution to η's produced at $E_{c.m.} = 4.42$ GeV.

In order to observe F^+'s decaying into a specific final state, events collected at 4.42 GeV were fit to the hypothesis $e^+e^- \rightarrow FF^* \rightarrow \pi\eta F\gamma$ where the $\eta \rightarrow \gamma\gamma$ candidates were constrained to the precise η mass, and the $\pi\eta$ system was constrained to the mass of the missing F. A scatter plot of the $\pi\eta$ mass versus its recoil mass is shown in Fig. 6.3 for events with an acceptable χ^2. There is a clustering of six events present in this plot which are F, F^* candidates where $M_F = 2.04 \pm 0.01$ GeV/c^2 and $M_{F^*} = 2.15 \pm 0.04$ GeV/c^2. These six events also tend to fit the hypothesis $e^+e^- \rightarrow F^*\bar{F}^*$, where $M_F = 2.00 \pm 0.04$ and $M_{F^*} = 2.1 \pm 0.02$ GeV. Here they take the average values and quote $M(F) =$

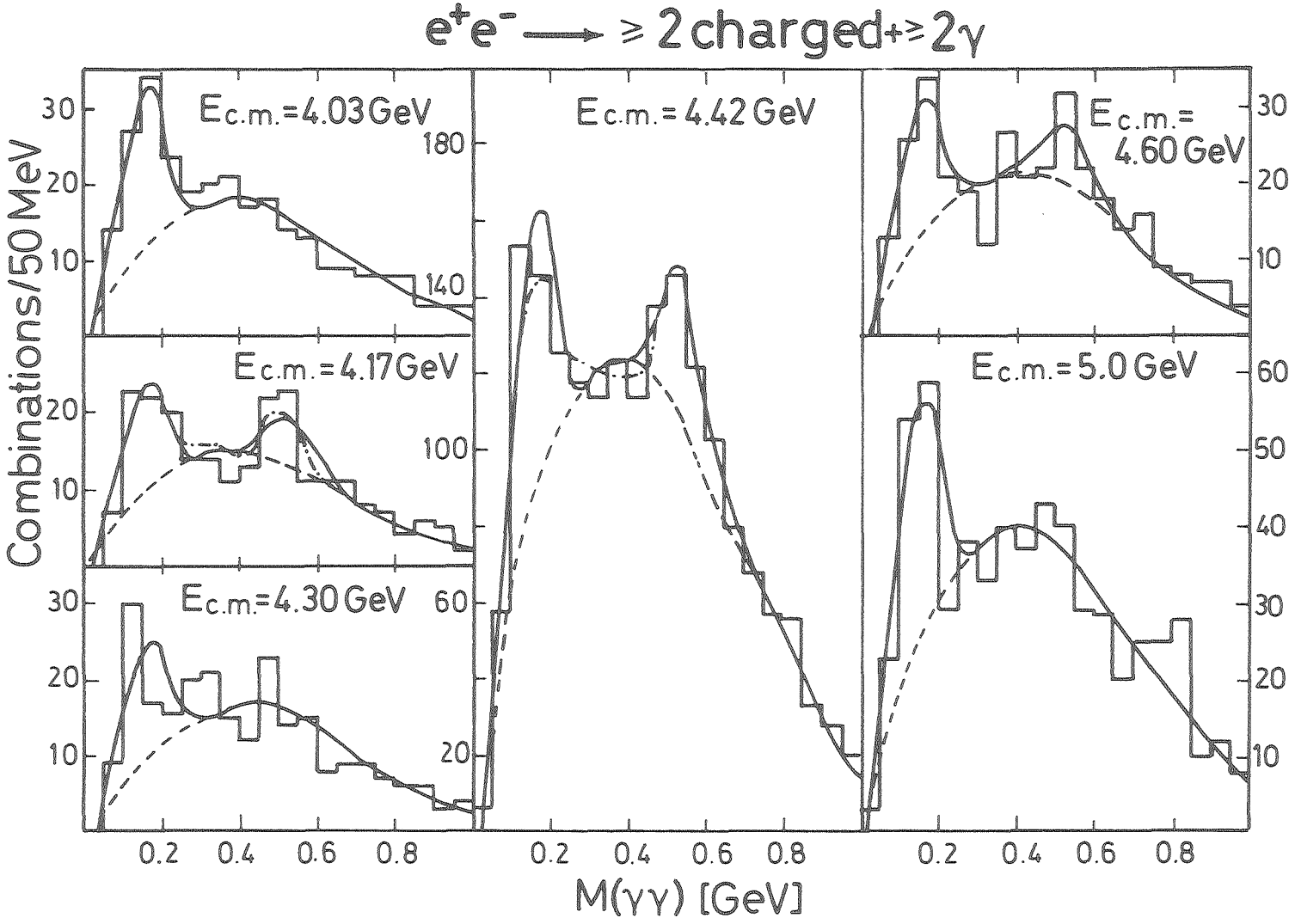

XBL 791-8185

Figure 6.1. DASP data on inclusive η production.

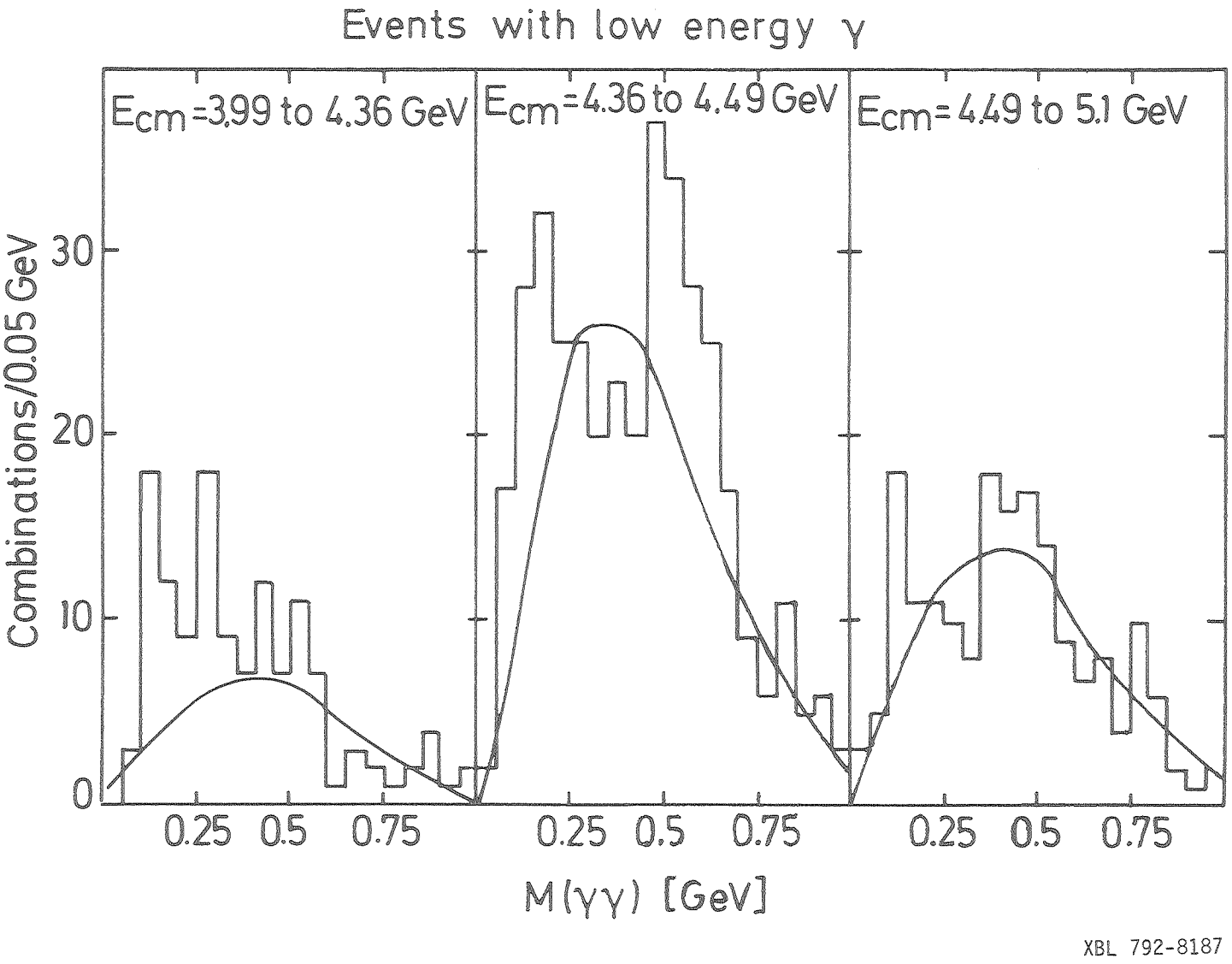

Figure 6.2. DASP data on η production for events with low energy γ-rays.

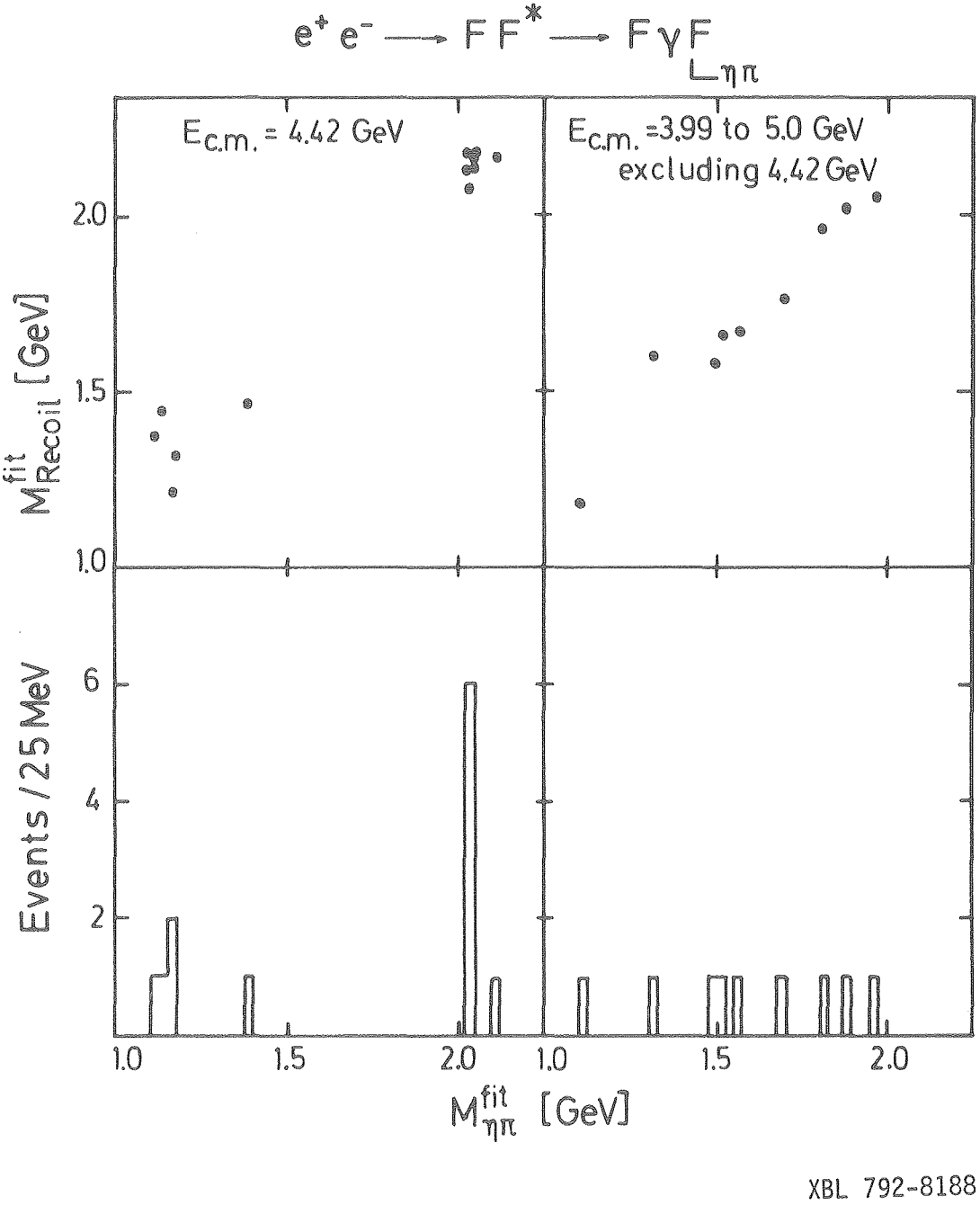

Figure 6.3. DASP data showing evidence for F production.

2.03 ± 0.06 GeV and $M(F^*) = 2.14 \pm 0.06$ GeV.

The six events imply $\sigma \cdot B(F^+ \to \eta\pi^+) = 0.41 \pm 0.18$ nb at the 4.42 resonance, a value which is close to the Mark II 95% C.L. upper limit of 0.26 nb at $E_{c.m.} = 4.42$ GeV and 0.33 nb at $E_{c.m.} = 4.16$ GeV. Clearly further work must be done to clarify the physics of the F.

ACKNOWLEDGMENTS

We want to thank Mrs. C. Frank-Dieterle for her help and meticulous care in preparing and compiling this manuscript.

This work was supported primarily by the U. S. Department under Contracts No. W-7405-ENG-48 (Lawrence Berkeley Laboratory) and DE-AC02-76ER01195 (University of Illinois).

We wish to thank the Staff of the Aspen Center for Physics for the hospitality extended to us during the Summer of 1979 while this review was being prepared in part.

Literature Cited

Abrams, G. S. et al. 1979. Phys. Rev. Lett. 43:481

Appelquist, T., Barnett, R. & Lane, K. 1978. Ann. Rev. Nucl. Part. Sci. 28:387

Aronson, S. H. et al. 1970. Phys. Rev. Lett. 25:1057

Aubert, J. J. 1974. Phys. Rev. Lett. 33:1404

Augustin, J.-E. et al. 1974. Phys. Rev. Lett. 33:1406

Bacino, W. et al. 1978. Phys. Rev. Lett. 40:671

Barbaro-Galtieri, A. 1968. Advances in Particle Physics, Vol. D, eds. R. Cool & R. Marshak, p. 193

Barbaro-Galtieri, A. 1978. Production and Decay of Charm Particles in e^+e^- Collisions, Lawrence Berkeley Laboratory Reports LBL-8537, LBL-9247 (1979)

Boyarski, A. M. et al. 1975. Phys. Rev. Lett. 34:1357

Brandelik, R. et al. 1979. Zeitschrift für Physik C, Particles and Fields 1:233

Braunschweig, W. et al. 1976. Phys. Lett. 63B:471

Bricman, C. et al. 1978. Phys. Lett. 75B:1

Burmester, J. et al. 1976. Phys. Lett. 64B:369

Camerini, U. et al. 1975. Phys. Rev. Lett. 35:483

Carithers, W. A. et al. 1973. Phys. Rev. Lett. 31:1025

Chinowsky, W. 1977. Ann. Rev. Nucl. Sci. 27:393

Clark, A. R. et al. 1971. Phys. Rev. Lett. 26:1667

Dorfan, J. 1979. Am. Phys. Soc. Meeting at McGill University, Montreal, Canada, SLAC-PUB-2429

Eichten, E. et al. 1975. Phys. Rev. Lett. 34:369

Ellis, J. 1974. Proc. XVII Int. Conf. High Energy Physics, London, p. IV-20

Fakirov, D. & Stech, B. 1978. Nucl. Phys. B133:315

Feldman, G. J. et al. 1977. Phys. Rev. Lett. 38:1313

Feldman, G. J. 1978. Proc. XIX Int. Conf. High Energy Physics, Tokyo, p. 777

Feller, J. M. 1979. Ph.D. thesis. University of California, Berkeley, LBL-9017

Feller, J. M. et al. 1978. Phys. Rev. Lett. 40:1677

Flügge, G. 1978. Proc. XIX Int. Conf. High Energy Physics, Tokyo, p. 793

Gaillard, M. K., Lee, B. W. & Rosner, J. 1975. Rev. Mod. Phys. 47:277

Gittleman, B. et al. 1975. Phys. Rev. Lett. 35:1616

Glashow, S. L., Illiopoulos, J. & Maiani, L. 1970. Phys. Rev. D2:1285

Goldhaber, G. et al. 1976. Phys. Rev. Lett. 37:255

Goldhaber, G. et al. 1977. Phys. Lett. 69B:503

Gottfried, K. 1978. Phys. Rev. Lett. 40:598

Harari, H. 1977. Proc. 1977 Summer Inst. on Part. Phys., Stanford Linear Accelerator Center, SLAC-204, p. 1

Herb, S. W. et al. 1977. Phys. Rev. Lett. 39:252

Iizuka, J. 1966. Suppl. Prog. Theor. Phys. 37:21

Jackson, J. D. & Scharre, D. L. 1975. Nucl. Instr. Meth. 128:13

Jean-Marie, B. et al. 1976. Phys. Rev. Lett. 36:291

Kirkby, J. 1979. Invited talk at the IX International Symposium on Lepton and Photon Interactions at High Energies, Batavia, IL

Klems, J. H., Hildebrand, R. H. & Stiening, R. 1970. Phys. Rev. Lett. 24:1086

Knapp, B. et al. 1975. Phys. Rev. Lett. 34:1040

Kobayashi, M. & Maskawa, T. 1973. Prog. Theor. Phys. 49:652

Lane, K. 1976. Phys. Rev. Lett. 37:477

Litke, A. et al. 1973. Phys. Rev. Lett. 30:1189

Lüth, V. 1979. Invited talk at IX Int. Symposium on Lepton and Photon Interactions at High Energies, Batavia, IL

Nguyen, H. K. et al. 1977. Phys. Rev. Lett. 39:262

Okubo, S. 1963. Phys. Rev. Lett. 5:165

Pais, A. & Treiman, S. B. 1977. Phys. Rev. D15:2529

Perez-y-Jorba, J. 1969. Proc. IV Int. Symp. on Electron and Photon Interactions at High Energies, Liverpool, p. 213

Perl, M. 1980. Ann. Rev. Nucl. Part. Sci. 30:in press

Peruzzi, I. et al. 1976. Phys. Rev. Lett. 37:569

Peruzzi, I. et al. 1977. Phys. Rev. Lett. 39:1301

Peruzzi, I. et al. 1978. Phys. Rev. D17:2901

Rapidis, P. A. et al. 1977. Phys. Rev. Lett. 39:526

Rapidis, P. A. 1979. Ph.D. thesis. Stanford University, SLAC-220

Richter, B. 1974. Proc. XVII Int. Conf. High Energy Physics, London, p. IV-37

Schindler, R. H. 1979. Ph.D. thesis. Stanford University, SLAC-219

Schindler, R. H. et al. 1980. Phys. Rev. D, in press

Schrock, R. E. & Wang, L. L. 1978. Phys. Rev. Lett. 41:1692

Schwitters, R. F. & Strauch, K. 1976. Ann. Rev. Nucl. Sci. 26:89

Siegrist, J. L. et al. 1976. Phys. Rev. Lett. 36:700

Tarnopolsky, G. et al. 1974. Phys. Rev. Lett. 32:432

Voyvodic, L. 1979. IX Int. Symp. on Lepton and Photon Interactions at High Energies, Batavia, IL

Vuillemin, V. et al. 1978. Phys. Rev. Lett. 41:1149

Wiik, B. H. & Wolf, G. 1978. DESY-78/23 (unpublished report).

Wiss, J. E. et al. 1976. Phys. Rev. Lett. 37:1531

Zweig, G. 1964. CERN-TH-401

Table 1.1. Quark quantum numbers.

Quark	u	d	s	c
Baryon number	1/3	1/3	1/3	1/3
Spin	1/2	1/2	1/2	1/2
Charge	+2/3	-1/3	-1/3	+2/3
Isospin	1/2	1/2	0	0
I_3	+1/2	-1/2	0	0
Strangeness	0	0	-1	0
Charm	0	0	0	1

Table 2.1. Resonance parameters for vector mesons.[a] Γ is the total width, Γ_e is the partial width to electron pairs, and B_e is the branching fraction to electron pairs.

State	Mass (MeV)	Γ (MeV)	Γ_e (keV)	B_e	Ref.
ρ	776 ± 3	155 ± 3	6.7 ± 0.8	$(4.3 \pm 0.5)10^{-5}$	b
ω	782.6 ± 0.3	10.1 ± 0.3	0.76 ± 0.17	$(7.6 \pm 1.7)10^{-5}$	b
φ	1019.6 ± 0.2	4.1 ± 0.2	1.31 ± 0.10	$(31 \pm 1)10^{-5}$	b
ψ	3095 ± 4	0.069 ± 0.015	4.8 ± 0.6	$(69 \pm 9)10^{-3}$	SLAC-LBL Mark I
ψ'	3684 ± 5	0.228 ± 0.056	2.1 ± 0.3	$(9.3 \pm 1.6)10^{-3}$	SLAC-LBL Mark I
ψ''	3772 ± 6	28 ± 5	0.35 ± 0.09	$(1.2 \pm 0.3)10^{-5}$	LGW
	3770 ± 6	24 ± 5	0.18 ± 0.06	$(0.7 \pm 0.2)10^{-5}$	DELCO
	3764 ± 5	24 ± 5	0.28 ± 0.05	$(1.2 \pm 0.2)10^{-5}$	Mark II
4.04[c]	4040 ± 10	52 ± 10	0.75 ± 0.10	$(1.4 \pm 0.4)10^{-5}$	DASP
4.16[c]	4159 ± 20	78 ± 10	0.77 ± 0.20	$(0.9 \pm 0.3)10^{-5}$	DASP
4.41	4414 ± 7	33 ± 10	0.44 ± 0.14	$(1.3 \pm 0.3)10^{-5}$	SLAC-LBL Mark I
Υ	9460 ± 10	~ 0.05	1.2 ± 0.2	$(2.6 \pm 1.4)10^{-2}$	d
Υ'	10016 ± 10	--	0.33 ± 0.10	--	d

[a] Other states have been reported between the φ and the ψ by experiments at Frascati and Orsay; we do not include them here.

[b] World averages compiled by the Particle Data Group (Bricman 1978).

[c] The SLAC-LBL and DELCO data do not separate this region into two states.

[d] Values for Υ and Υ' are averages of DASP II and DESY-Heidelberg as quoted by Flügge (1978).

Table 4.3. The branching ratio for $D \rightarrow e\nu X$.

Experiment	$E_{c.m.}$ (GeV)	Branching ratio (%)
DASP Wiik & Wolf 1978	3.99→ 4.08	8.0 ± 2.0
LGW Feller 1978	ψ"	7.2 ± 2.8
DELCO Kirkby 1979	ψ"	8.0 ± 1.5
Mark II Lüth 1979	ψ"	9.8 ± 3.0
	Average	8.0 ± 1.1

Table 4.4. Semileptonic decays of D^+ and D^o, Mark II data at the ψ".

Decay mode	# tags	# electrons	Background	Br(%)
$D^+ \rightarrow e^+$	295 ± 18	38	15 ± 1	15.8 ± 5.3
$\rightarrow e^-$		4	3.9 ± 0.5	
$D^o \rightarrow e^+$	480 ± 23	36	19 ± 1	5.2 ± 3.3
$\rightarrow e^-$		19	12 ± 1	

Table 4.5. The DELCO multi-prong electron data sample at the ψ".

Event description	Event topology		
	1 electron	2 electrons	2 electrons + "V" (K_s^o)
Observed	1416	21	8
Background	692	4.6	1.8
Charm signal	724	16.4	6.2

Table 5.1. Results from simultaneous fits to the D^0, D^+ momentum spectra at E_{cm} = 4.028 GeV, from Goldhaber (1977).

	Fit parameter	Normal fit	Isospin constrained fit	Estimated values
Masses in MeV/c^2	M_{D^0}	1864 (1.5)[a]	1862 (0.5)[a]	1863 ± 3[b]
	M_{D^+}	1874 (2.5)	1873 (2.0)	1874 ± 5
	$M_{D^{*0}}$	2006 (0.5)	2007 (0.5)	2006 ± 1.5
	$M_{D^{*+}}$	2009 (1.5)	2007 (0.5)	2008 ± 3
Branching ratios	$BR(D^{*0} \rightarrow \gamma D^0)$	0.45 (0.08)	0.75 (0.05)	0.55 ± 0.15
	$BR(D^{*+} \rightarrow \pi^+ D^0)$[c]	--	0.60 ± 0.15	--
	$\frac{BR(D^+ \rightarrow K^-\pi^+\pi^+)}{BR(D^0 \rightarrow K^-\pi^+)}$[c]	--	1.60 ± 0.60	--
D^0 source fractions	$D^0\bar{D}^0$	0.05 (0.03)	0.05 (0.02)	0.05 ± 0.03
	$D^0\bar{D}^{*0} + \bar{D}^0 D^{*0}$	0.42 (0.04)	0.34 (0.04)	0.38 ± 0.08
	$D^{*0}\bar{D}^{*0}$	0.47 (0.05)	0.32 (0.05)	0.40 ± 0.10
	$D^{*+}D^-$; $D^{*+} \rightarrow \pi^+ D^0$	0.03 (0.02)	0.09 (0.04)	0.06 ± 0.05
	$D^{*+}D^{*-}$; $D^{*+} \rightarrow \pi^+ D^0$	0.03 (0.03)	0.20 (0.07)	0.11 ± 0.10
D^+ source fractions	D^+D^-	0.09 (0.05)	0.09 (0.05)	0.09 ± 0.05
	$D^{*+}D^- + D^{*-}D^+$	0.65 (0.07)	0.58 (0.06)	0.62 ± 0.09
	$D^{*+}D^{*-}$	0.26 (0.08)	0.33 (0.08)	0.29 ± 0.10

[a] Quantities in parentheses are typical statistical errors for a single fit.

[b] Errors quoted include estimated systematic uncertainty.

[c] These values can only be obtained under the assumptions of the isospin constrained fit. The quoted errors do not reflect possible breakdown of these assumptions.

Table 5.2. Comparison of D results.

	SLAC-LBL (Mark I)	LGW	Mark II
M_{D^+}	1874 ± 5	1868.3 ± 0.9	--[a]
M_{D^0}	1863 ± 3	1863.3 ± 0.9	--[a]
$\frac{Br(D^+ \to K^- \pi^+ \pi^+)}{Br(D^0 \to K^- \pi^+)}$	1.6 ± 0.6	$\frac{3.9 \pm 1}{1.8 \pm 0.5} = 2.2 \pm 0.8$	$\frac{5.2 \pm 1.0}{2.8 \pm 0.5} = 1.9 \pm 0.5$

[a] Preliminary Mark II results on the D^+ and D^0 masses are in excellent agreement with the LGW data although final values are not available at this time.